UC San Diego

UC San Diego Electronic Theses and Dissertations

Title

Environmental Monitoring as a Means for Understanding SARS-CoV-2 Impacts on the Human and Built Environment Microbiome

Permalink

https://escholarship.org/uc/item/1rp6w4kc

Author

Cantu, Victor

Publication Date

2022

Peer reviewed|Thesis/dissertation

eScholarship.org Powered by the California Digital Library
University of California

UNIVERSITY OF CALIFORNIA SAN DIEGO

Environmental Monitoring as a Means for Understanding SARS-CoV-2 Impacts on the Human and Built Environment Microbiome

A dissertation submitted in partial satisfaction

of the requirements for the Doctor of Philosophy

in

Bioengineering

by

Victor J. Cantú

Committee in charge:

Professor Rob Knight, Chair
Professor Jack Gilbert
Professor Terry Hwa
Professor Bernhard Palsson
Professor Karsten Zengler

2022

Copyright

Victor J. Cantú, 2022

All Rights Reserved

The dissertation of Victor J. Cantú is approved, and it is acceptable in quality and form for publication on microfilm and electronically.

University of California San Diego

2022

DEDICATION

To the village supporting me, all of you.

EPIGRAPH

“Some of you guys need to read more like some of you guys are making the same mistakes as Odysseus”

— @mr_froodo

“…you gotta keep it tight baby boy.”

— @ojomoh_a

“[But then,] Victor happened.”

— @jbullockruns

TABLE OF CONTENTS

LIST OF FIGURES

LIST OF TABLES

ACKNOWLEDGMENTS

I make it no secret that I have struggled, both academically and personally, throughout grad school. It would be nearly impossible to name and adequately thank every single person that has helped me survive over these last few years but I'm gonna try.

I first need to thank every member of the Knight Lab who has sat with me while I worked through a problem and then sat with me again when I've forgotten what they said the first time (Smruthi Karthikeyan, Pedro Belda-Ferre, Jeff Chiu, Qiyun Zhu, Shi Huang, Tomasz Kosciolek, Se Jin Song, Antonio González Peña, Karenina Sanders, Rodolfo Antonio Salido Benítez, Celeste Allaband, Yoshiki Vazquez-Baeza, Peter De Hoff, Gibs Rahman, Lisa Marotz, Rob Mills, George Armstrong, Daniel Hakim, Jake Minich, Marcus Fedarko, Franck Lejzerowicz, Andre Mu, Jamie Morton, Cameron Martino, Holly Lutz, Justin Shaffer, Bod Estaki, Daniel McDonald, Jeff DeReus, Jon Sanders, Lingjing Serene Jiang). I would not have been able to get anywhere without the help of the highly capable scientists in the wet lab that kept my projects moving along and accommodated my requests when I was running behind schedule (Martin Casas Maya, Rebecca Tsai, Sawyer Farmer, MacKenzie Bryant, Madison Ambre, Greg Humphrey, Helena Tubb, Caitlin Tribelhorn, Tommy Valles). I also need to thank every admin in the Knight lab and bioengineering department (and really nearly every admin I've ever worked with) who patiently helped me through every tight - or missed - deadline (Yna Villanueva, Michiko Souza, Peggy Castaneda, Sarah Adams, Andrea Iriarte, Vanessa Hollingsworth, Jan Lenington). Thank you to the Rebecca Fielding-Miller lab that always reminded me how

important our work was (Rebecca Fielding-Miller, Carrissa Wijaya, Marlene Flores, Vinton Omaleki, Patricia Gonzalez-Zuniga). And finally thank you to each person that allowed me to be myself around them, who I could commiserate with, who listened to me when I was freaking out, and who celebrated my wins (Martin Casas Maya, Jeff Chiu, Smruthi Karthikeyan, Gail Ackerman, Rodolfo Antonio Salido Benítez, Pedro Belda-Ferre, Jerry Kennedy, Farhana Ali). Yall were really in the trenches with me and I wouldn't have made it through without you.

I really need to shout out my care team, Dr. Nancy Downs and Dr. Kristen Duarte. You got me across the finish line in one piece and helped me reach a place I never expected I could.

I would not have had the opportunity to earn a PhD if it were not for the people that taught and mentored me throughout my life. I wouldn't have made it to or through MIT without my teachers in middle-of-nowhere towns who gave me a strong academic foundation and ignited a passion for teaching (Mrs. Jamie Ballew, Mrs. Julie Bruce, Coach Chuck Anders). I'd also like to thank my mentors from MIT and Seres who helped me develop as a fledgling researcher and engineer (Tom McNicholas, Prof. Kris Prather, Noémie-Manuelle Dorval Courchesne, Manny Otero, Chris McChalicer). I also need to shout out the good work being done by the OEOP at MIT and the PATHs program here at UCSD for creating communities of mentors and mentees to which I am proud to belong.

My dear friends, I don't know where to begin; I am so lucky. Forest, I hope you know how much you mean to me. You believe in me more than you should. Steph, memories we made during your visits are some of my favorites of San Diego. Thanks for supporting me always even though my love language is being a total monster. And thanks

to both of you for letting me stay with you during the pandemic. I needed that. Mary, thank God you moved here when you did. I am in awe of you and your power. Your ability to talk me down from a ledge or help me untangle some current drama is superhuman. Jonathan, you're my tallest friend and the gentlest of giants/bbs. You made me feel cared for and listened to. You never let me talk badly about myself and I one day hope to support you even a fraction of the amount you've supported me. Clara, our kikis and pomodoro sessions sustained me; I will always treasure our little cafe dates. Jeff and Martin, I never felt that I was as good of a mentor to yall as I wanted to be, but you refused to let me feel that way and I thank you for that. I'm so proud of where you guys are now and excited to see where you're headed. Martin, I knew you were an incredible person from our first meeting but you continue to surprise me with just how great you are. Jeff, you're energy is unbeatable. You're so good and you never let me quit and I thank you for that. Michael, thanks for always lending me your car and thanks for always keeping your door open. One of the best parts of my day was walking out of my room, seeing the light at the end of the hall, and getting to talk to you about whatever nonsense was on my mind (and for bringing Crowley into my life). Cyrus and Lily, I've looked up to the both of you for so long and have become a better person because of it. I learned so much from living with you. You helped me find my footing and gave me my first home after leaving MIT. Janet and Tara, thanks for our phone calls. You always listened no matter how long I talked for. September, I like that we could always get weird together. Thanks for letting me listen to the songs you wrote and building a fort in the canyon with me. Alera, thanks for your baked goods and saying I made you feel like a dancer in Atlanta. And finally, Vivek. Thanks for sharing your Netflix login.

To my family, thank you. To my tíos, tías, and cousins, know that I've felt your support all the way over here and I'm excited to be moving back closer soon. To my grandmas, thank you for every single rosary you prayed for me, I felt your prayers, and through them, your love. To my brother, thank you for being an example I could look to; you've done more for me than you know. Dad, you've taught me so much. You've always made sure I know how proud of me you are and how much you love me - thank you, I love you. And to my mom. You've always put me first and anchored me when I felt lost. Thank you, and I love you.

And finally, Rob. Thank you. I owe this all to you. You have been beyond patient with me. You are the busiest man I know and still drop everything when I need help. _Thank you_

※※※

Chapter 1, in full, is a reprint of the material as it appears in *mSystems*, "Analysis of SARS-CoV-2 RNA Persistence across Indoor Surface Materials Reveals Best Practices for Environmental Monitoring Programs." Salido RA, Cantú VJ, Clark AE, Leibel SL, Foroughishafiei A, Saha A, Hakim A, Nouri A, Lastrella AL, Castro-Martínez A, Plascencia A, Kapadia BK, Xia B, Ruiz CA, Marotz CA, Maunder D, Lawrence ES, Smoot EW, Eisner E, Crescini ES, Kohn L, Franco Vargas L, Chacón M, Betty M, Machnicki M, Wu MY, Baer NA, Belda-Ferre P, De Hoff P, Seaver P, Ostrander RT, Tsai R, Sathe S, Aigner S, Morgan SC, Ngo TT, Barber T, Cheung W, Carlin AF, Yeo GW, Laurent LC, Fielding-Miller R, Knight R. The dissertation author was the primary investigator and first author of this paper.

Chapter 2, in full, is a reprint of the material as it appears in *mSystems*, “Sentinel Cards Provide Practical SARS-CoV-2 Monitoring in School Settings.” Cantú VJ, Sanders K, Belda-Ferre P, Salido RA, Tsai R, Austin B, Jordan W, Asudani M, Walster A, Magallanes CG, Valentine H, Manjoonian A, Wijaya C, Omaleki V, Aigner S, Baer NA, Betty M, Castro-Martínez A, Cheung W, De Hoff P, Eisner E, Hakim A, Lastrella AL, Lawrence ES, Ngo TT, Ostrander T, Plascencia A, Sathe S, Smoot EW, Carlin AF, Yeo GW, Laurent LC, Manlutac AL, Fielding-Miller R, Knight R. The dissertation author was the primary investigator and first author of this paper.

Chapter 3, in full, is a reprint of the material as it appears in *mSystems*, “Implementation of Practical Surface SARS-CoV-2 Surveillance in School Settings. ” Cantú VJ, Belda-Ferre P, Salido RA, Tsai R, Austin B, Jordan W, Asudani M, Walster A, Magallanes CG, Valentine H, Manjoonian A, Wijaya C, Omaleki V, Sanders K, Aigner S, Baer NA, Betty M, Castro-Martínez A, Cheung W, Crescini ES, De Hoff P, Eisner E, Hakim A, Kapadia B, Lastrella AL, Lawrence ES, Ngo TT, Ostrander T, Sathe S, Seaver P, Smoot EW, Carlin AF, Yeo GW, Laurent LC, Manlutac AL, Fielding-Miller R, Knight R. The dissertation author was the primary investigator and first author of this paper.

Chapter 4, in full, is a reprint of the material as it appears in *mSystems*, “SARS-CoV-2 Distribution in Residential Housing Suggests Contact Deposition and Correlates with Rothia sp..” Cantú VJ, Salido RA, Huang S, Rahman G, Tsai R, Valentine H, Magallanes CG, Aigner S, Baer NA, Barber T, Belda-Ferre P, Betty M, Bryant M, Casas Maya M, Castro-Martínez A, Chacón M, Cheung W, Crescini ES, De Hoff P, Eisner E, Farmer S, Hakim A, Kohn L, Lastrella AL, Lawrence ES, Morgan SC, Ngo TT, Nouri A, Plascencia A, Ruiz CA, Sathe S, Seaver P, Shwartz T, Smoot EW, Ostrander RT,

Valles T, Yeo GW, Laurent LC, Fielding-Miller R, Knight R. The dissertation author was the primary investigator and first author of this paper.

VITA

2016 B.S. in Chemical-Biological Engineering, Massachusetts Institute of Technology

2022 Ph. D. in Bioengineering, University of California San Diego

PUBLICATIONS

Author names marked with † indicate shared first co-authorship.

Cantú VJ†, Sanders K†, Belda-Ferre P, Salido RA, Tsai R, Austin B, Jordan W, Asudani M, Walster A, Magallanes CG, Valentine H, Manjoonian A, Wijaya C, Omaleki V, Aigner S, Baer NA, Betty M, Castro-Martínez A, Cheung W, De Hoff P, Eisner E, Hakim A, Lastrella AL, Lawrence ES, Ngo TT, Ostrander T, Plascencia A, Sathe S, Smoot EW, Carlin AF, Yeo GW, Laurent LC, Manlutac AL, Fielding-Miller R, Knight R. 2022. Sentinel Cards Provide Practical SARS-CoV-2 Monitoring in School Settings. mSystems 7.

Cantú VJ, Belda-Ferre P, Salido RA, Tsai R, Austin B, Jordan W, Asudani M, Walster A, Magallanes CG, Valentine H, Manjoonian A, Wijaya C, Omaleki V, Sanders K, Aigner S, Baer NA, Betty M, Castro-Martínez A, Cheung W, Crescini ES, De Hoff P, Eisner E, Hakim A, Kapadia B, Lastrella AL, Lawrence ES, Ngo TT, Ostrander T, Sathe S, Seaver P, Smoot EW, Carlin AF, Yeo GW, Laurent LC, Manlutac AL, Fielding-Miller R, Knight R. 2022. Implementation of Practical Surface SARS-CoV-2 Surveillance in School Settings. mSystems 7.

Cantú VJ†, Salido RA†, Huang S, Rahman G, Tsai R, Valentine H, Magallanes CG, Aigner S, Baer NA, Barber T, Belda-Ferre P, Betty M, Bryant M, Casas Maya M, Castro-Martínez A, Chacón M, Cheung W, Crescini ES, De Hoff P, Eisner E, Farmer S, Hakim A, Kohn L, Lastrella AL, Lawrence ES, Morgan SC, Ngo TT, Nouri A, Plascencia A, Ruiz CA, Sathe S, Seaver P, Shwartz T, Smoot EW, Ostrander RT, Valles T, Yeo GW, Laurent LC, Fielding-Miller R, Knight R. 2022. SARS-CoV-2 Distribution in Residential Housing Suggests Contact Deposition and Correlates with Rothia sp. . mSystems 7.

Fielding-Miller R, Karthikeyan S, Gaines T, Garfein RS, Salido R, **Cantú VJ**, Kohn L, Martin NK, Wijaya C, Flores M, Omaleki V, Majnoonian A, Gonzalez-Zuniga P, Nguyen M, Vo A V, Le T, Duong D, Hassani A, Dahl A, Tweeten S, Jepsen K, Henson B, Hakim A, Birmingham A, Mark AM, Nasamran CA, Rosenthal SB, Moshiri N, Fisch KM,

Humphrey G, Farmer S, Tubb HM, Valles T, Morris J, Kang J, Khaleghi B, Young C, Akel AD, Eilert S, Eno J, Curewitz K, Laurent LC, Rosing T, SEARCH, Knight R. 2021. Wastewater and surface monitoring to detect COVID-19 in elementary school settings: The Safer at School Early Alert project. medRxiv Prepr Serv Heal Sci https://doi.org/10.1101/2021.10.19.21265226.

Huang S, Jiang S, Huo D, Allaband C, Estaki M, **Cantú VJ**, Belda-Ferre P, Vázquez-Baeza Y, Zhu Q, Ma C, Li C, Zarrinpar A, Liu YY, Knight R, Zhang J. 2021. Candidate probiotic Lactiplantibacillus plantarum HNU082 rapidly and convergently evolves within human, mice, and zebrafish gut but differentially influences the resident microbiome. Microbiome 9:1–17.

Salido RA†, **Cantú VJ†**, Clark AE, Leibel SL, Foroughishafiei A, Saha A, Hakim A, Nouri A, Lastrella AL, Castro-Martínez A, Plascencia A, Kapadia BK, Xia B, Ruiz CA, Marotz CA, Maunder D, Lawrence ES, Smoot EW, Eisner E, Crescini ES, Kohn L, Franco Vargas L, Chacón M, Betty M, Machnicki M, Wu MY, Baer NA, Belda-Ferre P, De Hoff P, Seaver P, Ostrander RT, Tsai R, Sathe S, Aigner S, Morgan SC, Ngo TT, Barber T, Cheung W, Carlin AF, Yeo GW, Laurent LC, Fielding-Miller R, Knight R. 2021. Analysis of SARS-CoV-2 RNA Persistence across Indoor Surface Materials Reveals Best Practices for Environmental Monitoring Programs. mSystems 6.

Yoo BB, Griffiths JA, Thuy-Boun P, **Cantú VJ**, Weldon K, Challis C, Sweredoski MJ, Chan KY, Thron TM, Sharon G, Moradian A, Humphrey G, Zhu Q, Shaffer J, Wolan DW, Dorrestein PC, Knight R, Gradinaru V, Mazmanian SK. 2021. Neuronal Activation of the Gastrointestinal Tract Shapes the Gut Environment in Mice. bioRxiv 2021.04.12.439539.

Zhu Q, Hou Q, Huang S, Ou Q, Huo D, Vázquez-Baeza Y, Cen C, **Cantú VJ**, Estaki M, Chang H, Belda-Ferre P, Kim HC, Chen K, Knight R, Zhang J. 2021. Compositional and genetic alterations in Graves' disease gut microbiome reveal specific diagnostic biomarkers. ISME J 2021 1511 15:3399–3411.

ABSTRACT OF THE DISSERTATION

Environmental Monitoring as a Means for Understanding SARS-CoV-2 Impacts on the Human and Built Environment Microbiome

by

Victor J. Cantú

Doctor of Philosophy in Bioengineering

University of California San Diego, 2022

Professor Rob Knight, Chair

Monitoring severe acute respiratory syndrome coronavirus 2 (SARS-CoV-2) on surfaces is emerging as an important tool for identifying past exposure to individuals shedding viral RNA. Because humans are a dominant source of microbial input into built environment samples, and because SARS-CoV-2 is known to modify the human microbiome, better technologies for reading out both SARS-CoV-2 specifically and the microbiome in general are required. Because the Knight lab has focused on obtaining

bacterial, archaeal, and fungal communities from built environment biospecimens for the last 15 years, and because of my own experience working with surface samples from schools as part of the SASEA (Safer at School Early Alert) program, my thesis focuses on improving methods for SARS-CoV-2 detection from built environment specimens, and relating these results to the rest of the microbiome as determined by more established methods such as 16S rRNA amplicon sequencing using the Earth Microbiome Project protocols, developed in the Knight lab.

In order to develop practical methods for obtaining SARS-CoV-2 loads on surfaces that are applicable not only to schools (the focus of SASEA) but to other settings including residential elder care, hospitals, and prisons, my thesis takes a systems engineering approach to surface sampling. Specifically, we need to know how to sample (including solving issues with signal persistence), how to perform the biospecimen collection and molecular assays, and where in the environment to sample to optimize signal.

Chapter 1. Analysis of SARS-CoV2 RNA persistence across indoor surface materials reveals best practices for environmental monitoring programs

Abstract

Environmental monitoring in public spaces can be used to identify surfaces contaminated by persons with COVID-19 and inform appropriate infection mitigation responses. Research groups have reported detection of Severe Acute Respiratory Syndrome Coronavirus 2 (SARS-CoV-2) on surfaces days or weeks after the virus has been deposited, making it difficult to estimate when an infected individual may have shed virus onto a SARS-CoV-2 positive surface, which in turn complicates the process of establishing effective quarantine measures. In this study, we determined that reverse transcription-quantitative polymerase chain reaction (RT-qPCR) detection of viral RNA from heat-inactivated particles experiences minimal decay over seven days of monitoring on eight out of nine surfaces tested. The properties of the studied surfaces result in RT-qPCR signatures that can be segregated into two material categories, rough and smooth, where smooth surfaces have a lower limit of detection. RT-qPCR signal intensity (average quantification cycle (Cq)) can be correlated to surface viral load using only one linear regression model per material category. The same experiment was performed with untreated viral particles on one surface from each category, with essentially identical results. The stability of RT-qPCR viral signal demonstrates the need to clean monitored

surfaces after sampling to establish temporal resolution. Additionally, these findings can be used to minimize the number of materials and timepoints tested and allow for the use of heat-inactivated viral particles when optimizing environmental monitoring methods.

Importance

Environmental monitoring is an important tool for public health surveillance, particularly in settings with low rates of diagnostic testing. Time between sampling public environments, such as hospitals or schools, and notifying stakeholders of the results should be minimal, allowing decisions to be made towards containing outbreaks of coronavirus disease 2019 (COVID-19). The Safer At School Early Alert program (SASEA) [1], a large-scale environmental monitoring effort in elementary school and child care settings, has processed >13,000 surface samples for SARS-CoV-2, detecting viral signals from 574 samples. However, consecutive detection events necessitated the present study to establish appropriate response practices around persistent viral signals on classroom surfaces. Other research groups and clinical labs developing environmental monitoring methods may need to establish their own correlation between RT-qPCR results and viral load, but this work provides evidence justifying simplified experimental designs, like reduced testing materials and the use of heat-inactivated viral particles.

1.1. Introduction

Development and characterization of methods for environmental monitoring of Severe Acute Respiratory Syndrome Coronavirus 2 (SARS-CoV-2) remain important

areas of research for identifying and mitigating potential outbreaks as the global pandemic continues. Environmental monitoring offers indirect detection of possibly infectious individuals through noninvasive sampling. In spaces with relatively consistent occupants, detection of SARS-CoV-2 from environmental samples can help identify COVID-19-infected individuals, ideally before further transmission. Environmental monitoring can also alert public health leadership to the potential presence of an infection even in settings with low diagnostic testing uptake, allowing for the implementation of enhanced non-pharmaceutical interventions (i.e., double masking, increased hand hygiene, improved ventilation efforts) even in the absence of positive diagnostic tests.

SARS-CoV-2 particles are shed by symptomatic and asymptomatic carriers [2] and have been detected on various surfaces [3, 4, 5, 6]. Viral signatures have been demonstrated to persist up to 4 weeks in bulk floor dust collected from a room with a quarantined individual [6]. Previous environmental monitoring studies have detected SARS-CoV-2 on surfaces contaminated by infected individuals in hospitals and congregate care facilities [7, 8, 9, 10, 11]. Thus, indoor surface sampling can be valuable for detection of infected persons indoors, where transmission risk is highest [12]. The Safer At School Early Alert program (SASEA) [1] uses environmental monitoring and collected over 13,000 surface swabs, but we need more information to clarify what these data are telling us over time.

We sought to characterize temporal dynamics underlying detection of SARS-CoV-2 signals from surface swabs from a variety of common indoor surface types using Reverse Transcription-quantitative Polymerase Chain Reaction (RT-qPCR). The Centers for Disease Control and Prevention (CDC) maintains that the risk of fomite transmission

of SARS-CoV-2 is low [13]. This study makes no claims of attempting to understand the possibility of or mechanisms behind infection of virus transmitted by fomites, but rather on whether and how negative and positive RT-qPCR detection from surface swabs can enable decision-making in outbreak mitigation, focused clinical testing of individuals, and safe reopening of high-traffic, public spaces.

We used RT-qPCR to detect heat-inactivated viral particles on nine surface materials, and monitored the persistence of the heat-inactivated virus for 7 days. Each material - acrylic, steel, glass, ceramic tile, melamine-finished particleboard (MFP), painted drywall, vinyl flooring, and two different carpets (olefin and polyester) - was divided into 5 cm by 5 cm grids, and each 25 cm2 square surface of the grid was inoculated with 10 µL of either a dilution series of heat-inactivated SARS-CoV-2 particles or water. The 8-point dilution series was based on viral genomic equivalents (GEs) as measured by digital droplet PCR (ddPCR). The inoculum dried for 1 hr before swabbing. Every 24 hours post-inoculation an unswabbed section of each material grid was sampled, for a total of seven days including the initial post-inoculation swab.

To determine whether use of heat-inactivated viral particles in testing and validating environmental monitoring methods reflects results obtained using untreated virus, we compared detection of heat-inactivated SARS-CoV-2 (strain WA-1, SA-WA1/2020) and of authentic, untreatedSARS-CoV-2 (variant of concern Beta, isolate B.1.351, hCoV-19/USA/MD-HP01542/2021) on two materials under biosafety level 3 (BSL-3) conditions.

1.2. Results

Linear regression of signal intensity (average Cq of viral gene calls) on elapsed time since inoculation (days) for each dilution showed minimal decay of viral RNA on 8 of 9 surface types over 6 days (Fig. 1.1). The average decay slope for each surface type (m-bar) did not differ significantly from zero (mean=0.0407, s.d.=0.210). RT-qPCR signal decayed with time only on glass (m-bar=0.401, s.d.=0.212, differing from the population mean by >1.5 standard deviations).

A two-way repeated measure analysis of variance (ANOVA) on viral signal intensity (average Cq) revealed that surface type explains more observed variation in Cq than does time since inoculation at the highest concentration (5x105 GE's) (Fig. 1.2A). A Kruskal-Wallis H test confirmed that mean Cq's differ significantly across surface types (H=60.86, p=2.49x10^-9)(Fig. 1.2B), but not across days since inoculation (H=1.34, p=0.97)(Fig. 1.2C). Pairwise Mann-Whitney U tests comparing ranked values of Cq's from samples grouped by surface type highlight that both carpet materials (olefin and polyester) are significantly different, after correcting for multiple comparisons (FDR-Benjamini/Hochberg, alpha=0.005), from all other surfaces, but not from each other (Fig. 1.2B). Other pairwise, significant differences between materials are summarized in Supplementary Table S1. A clustermap of the U statistic from the pairwise comparisons effectively clusters samples by material properties, with rough surfaces clustering away from smooth ones (Fig. 1.2D).

Figure 1.1. Scatterplots showing the average Cq of RT-qPCR viral gene calls for corresponding heat-inactivated viral spike-in over seven days. alongside each surface type.alongside each surface type.

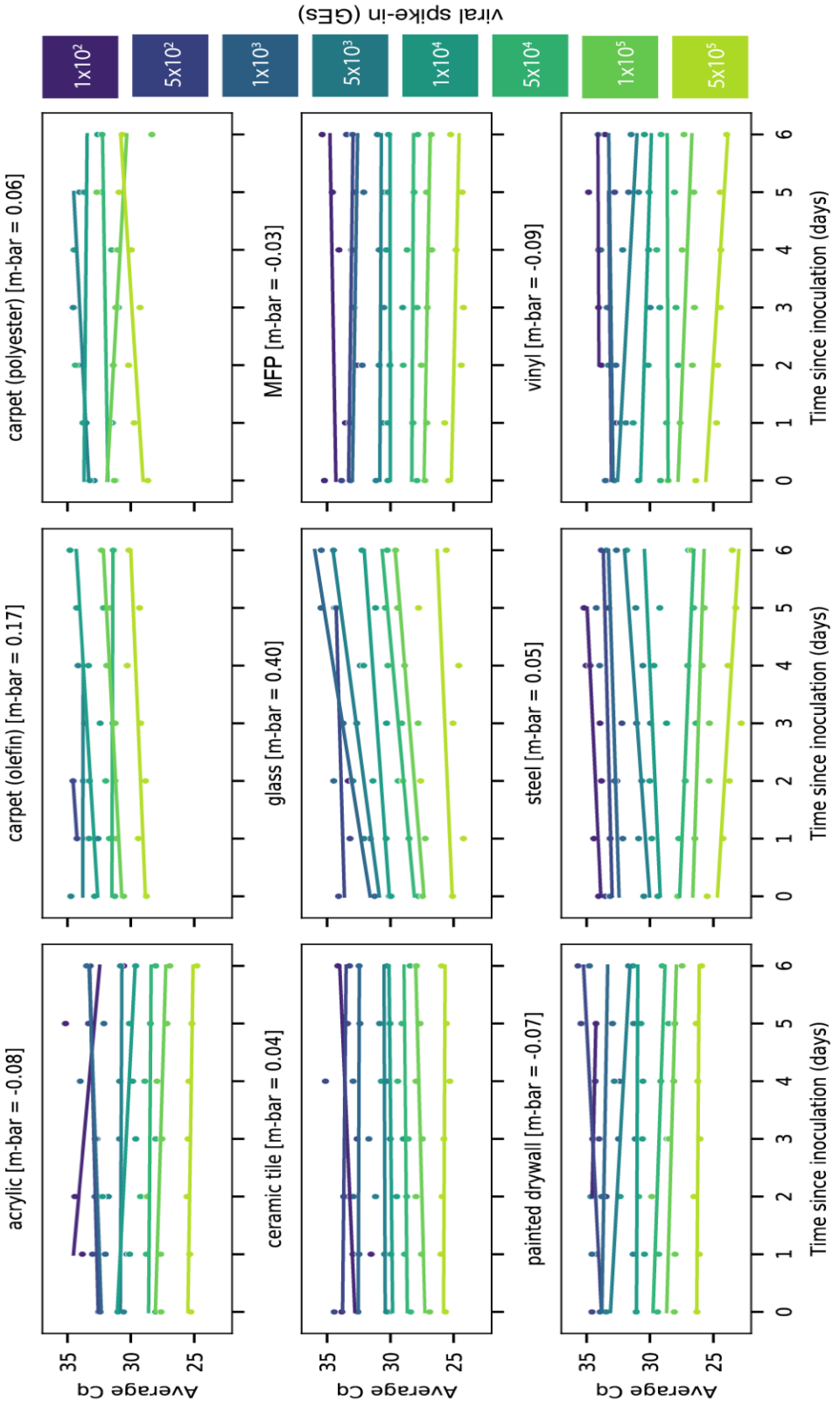
viral spike-in (GEs)
1x10²
5x10²
1x10³
5x10³
1x10⁴
5x10⁴
1x10⁵
5x10⁵
acrylic [m-bar = -0.08]
carpet (olefin) [m-bar = 0.17]
carpet (polyester) [m-bar = 0.06]
ceramic tile [m-bar = 0.04]
glass [m-bar = 0.40]
MFP [m-bar = -0.03]
painted drywall [m-bar = -0.07]
steel [m-bar = 0.05]
vinyl [m-bar = -0.09]
Average Cq
Time since inoculation (days)

Figure 1.2. Signal persistence of SARS-CoV-2 across material types.
(A-C) 3D scatterplots showing distribution of average Cq of viral gene calls over seven days for nine different surfaces inoculated with 5x105 GEs (nine surfaces for heat-inactivated virus [circles], two (acrylic and olefin carpet) for infectious [diamonds]). The distribution of Cq's differs significantly across surface types (B), but not across days since inoculation (C). (D) Clustermap of the U statistic from pairwise Mann-Whitney U tests between surface types. (E-F) Standard curves relating surface viral load (log2 spike-in) to average Cq across all time-points for smooth (E) and rough (F) surface types.

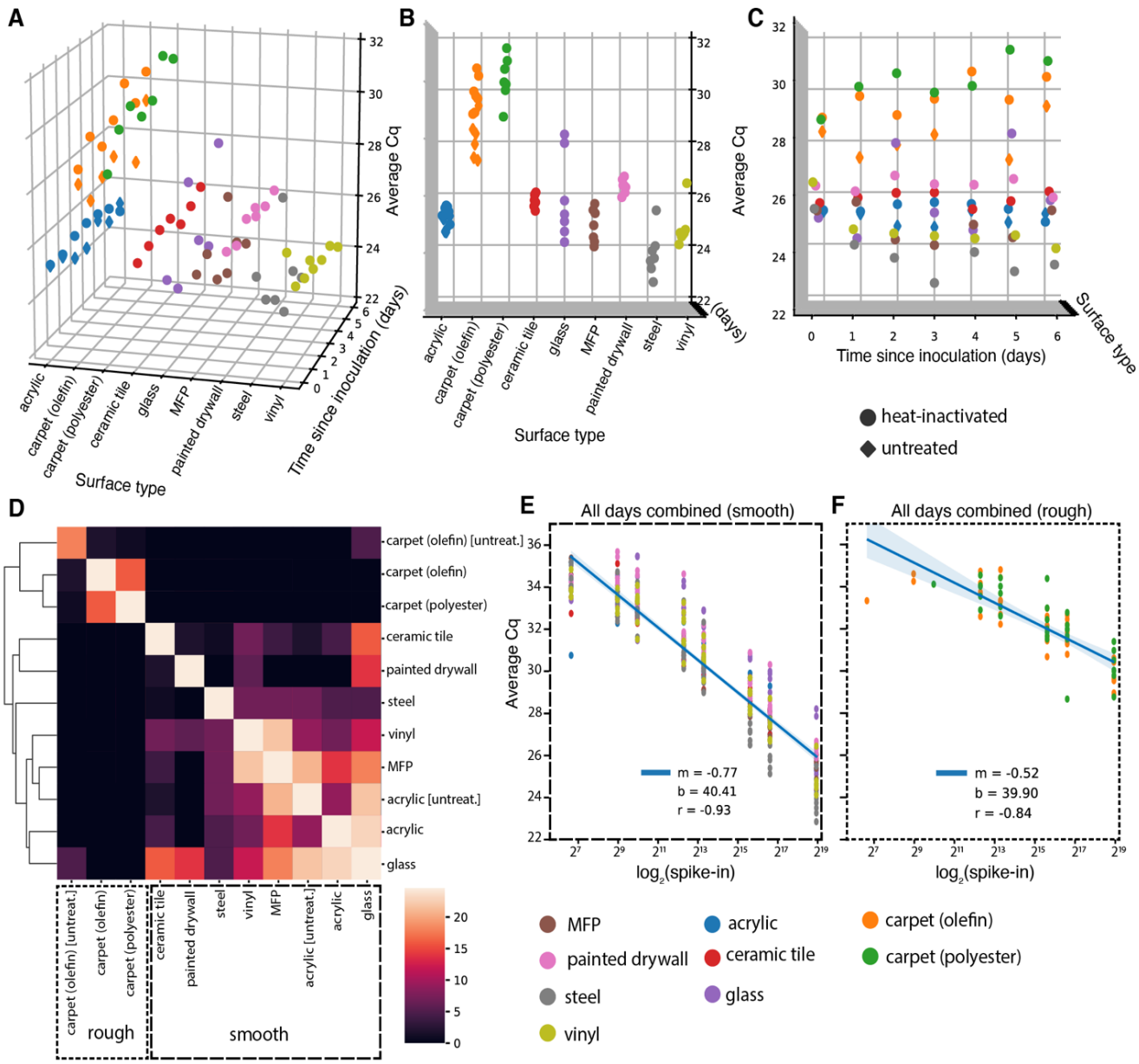
A
B
C
Average Cq
Surface type
Time since inoculation (days)
acrylic
carpet (olefin)
carpet (polyester)
ceramic tile
glass
MFP
painted drywall
steel
vinyl
heat-inactivated
untreated
D
carpet (olefin) [untreat.]
acrylic [untreat.]
rough
smooth
E
All days combined (smooth)
m = -0.77
b = 40.41
r = -0.93
log2(spike-in)
F
All days combined (rough)
m = -0.52
b = 39.90
r = -0.84

Because RT-qPCR signal intensity for most surfaces was time invariant, time-collapsed linear regression models relating viral spike-in concentration (log2 spike-in) to average Cq act as standard curves for estimating viral load on different monitored surfaces from Cq. After segregating samples based on the qualitative material categories of smooth or rough, linear regressions aggregating all timepoints yielded one standard curve for smooth surfaces (m=-0.77, b=40.41, r=-0.93)(Fig. 1.2E) and another for rough surfaces (m=-0.52, b=39.90, r=-0.84)(Fig. 1.2F). The reduced slope of the latter curve stems from higher loss of spiked-in viral signal to the rough surface matrix.

To ensure that viral signal stability was not a consequence of selection for resilient viral particles through heat inactivation, we repeated a subset of experiments using infectious virus (untreated) in a BSL-3 laboratory using the B.1.351/Beta variant of SARS-CoV-2 originally identified in South Africa. Due to space limitations in the BSL-3 facility, the untreated virus experiment only included two surface types, acrylic and carpet (olefin), but used the same dilution series and sampling plan.

Results from untreated and heat-inactivated virus are concordant. Untreated virus samples cluster with respect to surface type rather than virion status (heat-inactivated or untreated) (Figure. 2D). When evaluating acrylic and carpet (olefin) samples alone, a Kruskal-Wallis H test shows significant differences in the means of Cq's across all groups when samples are grouped by surface type (H=16.37, p=0.00095) (Fig. AA.1.S1A), but not when grouped by virion status (H=1.96, p=.161) (Fig. AA.1.S1B). Furthermore, linear regression on Cq from paired samples between the heat-inactivated and untreated virus experiments show nearly exact correlation despite the use of different variants (m=1.05, r=0.97) (Fig. AA.1.S1C).

1.3. Discussion

We show that detecting SARS-CoV-2 RNA on indoor surfaces in environments potentially exposed to COVID-19 infected individuals is effective across a variety of surfaces and a range of initial viral loads. Our swabbing and RT-qPCR methods have greater sensitivity from smooth surfaces (such as MFP - commonly found on desktops - or vinyl flooring) than rough surfaces (carpet). The stability of the viral signal across time limits the ability to estimate when the surface was inoculated, but demonstrates that signal can be detected a week post-exposure. There is a possibility that viral signal could decay over a longer period of time, but because the motivation behind this study was to improve temporal resolution over shorter periods, this was beyond the scope of the present work. To improve temporal resolution, surfaces swabbed for environmental monitoring should be cleaned with soap and water, following CDC recommendations [14], in order to remove viral signals [13]. Previous work with comparable methods for SARS-CoV-2 detection from surfaces demonstrated that washing contaminated objects with household dishwashing detergent for ≥ 1 minute removed enough viral RNA traces so that only 20% of the severely contaminated objects had detectable viral RNA. Furthermore, the average viral load of the washed surfaces was reduced by ~2.5 Cq's in comparison to untreated objects [15]. Thus, cleaning monitored surfaces with soap and water improves the probability of distinction between persistent or separate exposures in subsequent SARS-CoV-2 detection events.

Although direct inoculation of surfaces with viral particles does not represent interaction with an infected individual in a real-world scenario, we do directly show that

untreated and heat-inactivated SARS-CoV-2 particles have similar detectability and stability across surface types. These findings allow the use of heat-inactivated particles in testing and validating environmental monitoring methods, and remove the burden of performing such experiments in BSL-3 laboratories.

1.4. Acknowledgements

We thank our partner schools and citizen scientists at 15 sites across 5 districts in San Diego county. This research was supported by NIH grant (K08AI130381) and a Career Award for Medical Scientists from the Burroughs Wellcome Fund to AFC, NIH grant (K01MH112436) to RFM, and the County of San Diego Health and Human Services Agency (Contract 563236). This work was performed with the support of the Genomics and Sequencing Core at the UC San Diego Center for AIDS Research (P30 AI036214), the VA San Diego Healthcare System, and the Veterans Medical Research Foundation. The following reagent was deposited by the Centers for Disease Control and Prevention and obtained through BEI Resources, NIAID, NIH: SARS-Related Coronavirus 2, Isolate USA-WA1/2020, NR-52281. The following reagent was obtained through BEI Resources, NIAID, NIH: SARS-Related Coronavirus 2, Isolate hCoV-19/South Africa/KRISP-K005325/2020, NR-54009, contributed by Alex Sigal and Tulio de Oliveira.

Chapter 1, in full, is a reprint of the material as it appears in *mSystems*, “Analysis of SARS-CoV-2 RNA Persistence across Indoor Surface Materials Reveals Best Practices for Environmental Monitoring Programs.” Salido RA, Cantú VJ, *et al*. The dissertation author was the primary investigator and first author of this paper.

1.5. References

1. SASEA System – Safer At School Early Alert. Available at: https://saseasystem.org/. (Accessed: 1st July 2021)

2. Meyerowitz EA, Richterman A, Gandhi RT, Sax PE. 2021. *Transmission of SARS-CoV-2: A Review of Viral, Host, and Environmental Factors.* Ann Intern Med. NLM (Medline).

3. Parker CW, Singh N, Tighe S, Blachowicz A, Wood JM, Seuylemezian A, Vaishampayan P, Urbaniak C, Hendrickson R, Laaguiby P, Clark K, Clement BG, O'Hara NB, Couto-Rodriguez M, Bezdan D, Mason CE, Venkateswaran K. 2020. *End-to-End Protocol for the Detection of SARS-CoV-2 from Built Environments.* mSystems 5.

4. van Doremalen N, Bushmaker T, Morris DH, Holbrook MG, Gamble A, Williamson BN, Tamin A, Harcourt JL, Thornburg NJ, Gerber SI, Lloyd-Smith JO, de Wit E, Munster VJ. 2020. *Aerosol and Surface Stability of SARS-CoV-2 as Compared with SARS-CoV-1.* N Engl J Med 382:1564–1567.

5. Chin AWH, Chu JTS, Perera MRA, Hui KPY, Yen H-L, Chan MCW, Peiris M, Poon LLM. 2020. *Stability of SARS-CoV-2 in different environmental conditions.* The Lancet Microbe 1:e10.

6. Harbourt DE, Haddow AD, Piper AE, Bloomfield H, Kearney BJ, Fetterer D, Gibson K, Minogue T. 2020. *Modeling the stability of severe acute respiratory syndrome coronavirus 2 (SARS-CoV-2) on skin, currency, and clothing.* PLoS Negl Trop Dis 14:e0008831.

7. Renninger N, Nastasi N, Bope A, Cochran SJ, Haines SR, Balasubrahmaniam N, Stuart K, Bivins A, Bibby K, Hull NM, Dannemiller KC. 2021. *Indoor Dust as a Matrix for Surveillance of COVID-19*. mSystems 6.

8. Ye G, Lin H, Chen S, Wang S, Zeng Z, Wang W, Zhang S, Rebmann T, Li Y, Pan Z, Yang Z, Wang Y, Wang F, Qian Z, Wang X. 2020. *Environmental contamination of SARS-CoV-2 in healthcare premises.* J Infect 81:e1–e5.

9. Ben-Shmuel A, Brosh-Nissimov T, Glinert I, Bar-David E, Sittner A, Poni R, Cohen R, Achdout H, Tamir H, Yahalom-Ronen Y, Politi B, Melamed S, Vitner E, Cherry L, Israeli O, Beth-Din A, Paran N, Israely T, Yitzhaki S, Levy H, Weiss S. 2020. *Detection and infectivity potential of severe acute respiratory syndrome coronavirus 2 (SARS-CoV-2) environmental contamination in isolation units and quarantine facilities.* Clin Microbiol Infect 26:1658–1662.

10. Jiang FC, Jiang XL, Wang ZG, Meng ZH, Shao SF, Anderson BD, Ma MJ. 2020. *Detection of severe acute respiratory syndrome coronavirus 2 RNA on surfaces in quarantine rooms.* Emerg Infect Dis 26:2162–2164.

11. Marotz C, Belda-Ferre P, Ali F, Das P, Huang S, Cantrell K, Jiang L, Martino C, Diner RE, Rahman G, McDonald D, Armstrong G, Kodera S, Donato S, Ecklu-Mensah G, Gottel N, Salas Garcia MC, Chiang LY, Salido RA, Shaffer JP, Bryant MK, Sanders K, Humphrey G, Ackermann G, Haiminen N, Beck KL, Kim HC, Carrieri AP, Parida L, Vázquez-Baeza Y, Torriani FJ, Knight R, Gilbert J, Sweeney DA, Allard SM. 2021. *SARS-CoV-2 detection status associates with bacterial community composition in patients and the hospital environment.* Microbiome 9:1–15.

12. Coronavirus (COVID-19) frequently asked questions | CDC. Available at: https://www.cdc.gov/coronavirus/2019-ncov/faq.html#Spread. (Accessed: 1st July 2021)

13. Science Brief: SARS-CoV-2 and Surface (Fomite) Transmission for Indoor Community Environments | CDC. Available at: https://www.cdc.gov/coronavirus/2019-ncov/more/science-and-research/surface-transmission.html. (Accessed: 1st July 2021)

14. Cleaning and Disinfecting Your Home | CDC. Available at: https://www.cdc.gov/coronavirus/2019-ncov/prevent-getting-sick/disinfecting-your-home.html. (Accessed: 10th September 2021)

15. Salido RA, Morgan SC, Rojas MI, Magallanes CG, Marotz C, DeHoff P, Belda-Ferre P, Aigner S, Kado DM, Yeo GW, Gilbert JA, Laurent L, Rohwer F, Knight R. 2020. *Handwashing and Detergent Treatment Greatly Reduce SARS-CoV-2 Viral Load on Halloween Candy Handled by COVID-19 Patients.* mSystems 5.

Chapter 2. Sentinel Cards Provide Practical SARS-CoV-2 Monitoring in School Settings

Abstract

Accurate, high-resolution environmental monitoring of SARS-CoV-2 traces indoors through sentinel cards is a promising approach to help students safely return to in-person learning. Because SARS-CoV-2 RNA can persist for up to a week on several indoor surface materials, there is a need for increased temporal resolution to determine whether consecutive surface positives arise from new infection events or continue to report past events. Cleaning sentinel cards after sampling would provide the needed resolution, but might interfere with assay performance. We tested the effect of three cleaning solutions (BZK wipes, Wet Wipes, RNase Away) at three different viral loads: “high” (4×10^4 GE/mL), “medium” (1×10^4 GE/mL), and “low” (2.5×10^3 GE/mL). RNase Away, chosen as a positive control, was the most effective cleaning solution on all three viral loads. Wet Wipes were found to be more effective than BZK wipes in the medium viral load condition. The low viral load condition was easily reset with all three cleaning solutions. These findings will enable temporal SARS-CoV-2 monitoring in indoor environments where transmission risk of the virus is high and the need to avoid individual-level sampling for privacy or compliance reasons exists.

Importance

Because SARS-CoV-2, the virus that causes COVID-19, persists on surfaces, testing swabs taken from surfaces is useful as a monitoring tool. This approach is especially valuable in school settings, where there are cost and privacy concerns that are eliminated by taking a single sample from a classroom. However, the virus persists for days to weeks on surface samples, so it is impossible to tell whether positive detection events on consecutive days are persistent signal or new infectious cases, and therefore whether the positive individuals have been successfully removed from the classroom. We compare several methods for cleaning “sentinel cards” to show that this approach can be used to identify new SARS-CoV-2 signals day to day. The results are important for determining how to monitor classrooms and other indoor environments for SARS-CoV-2 virus.

2.1. Introduction

For the last two years, the SARS-CoV-2 pandemic has disrupted lives and caused millions of deaths globally. Due to the high risk of virus transmission in indoor settings, schools have been forced to convert to remote learning [1]. Although remote learning can be convenient for some, not every child has access to a stable internet connection and a supportive, quiet learning environment [2,3]. Therefore, most child health authorities are recommending a return to in-person learning, if it can be conducted safely [4]. Effective SARS-CoV-2 monitoring is crucial to allow for in-person learning to resume safely and widely [5], with the goal of restoring education equity. However, performing daily nasal

swabs to monitor the spread of the disease has high financial and labor costs, and often runs into difficulties with consent and reporting of results to relevant public health authorities.

Wastewater and environmental monitoring strategies have been developed [6-8] and implemented [9] as a means of circumventing clinical swabs. We have already demonstrated that viral signals from COVID-19 patients in indoor environments commonly accumulate on high-touch surfaces and the floors in front of features with high interaction times [8]. Additionally, SARS-CoV-2 RNA has been demonstrated to persist for up to a week on several indoor surface materials [7, 10], making it difficult to understand exactly when an infected individual came into contact with a surface or if consecutive positives are from new deposition events. Thus, an effective post-sampling cleaning procedure needs to be established in order to increase temporal resolution and ensure that consecutive positives are from new infection events.

2.2. Methods

To increase the temporal resolution of proven environmental pipelines [9,11], we tested resetting SARS-CoV-2 RNA signal with a mock sentinel surface. Here, a sentinel surface is a surface used as an environmental monitoring tool for detecting whether or not an infected individual was recently present in an indoor space. The mock sentinel surfaces we used were 100 cm2 laminated cards. The sentinel cards were inoculated with 10 µL of a dilution series of heat-inactivated SARS-CoV-2 particles (strain WA-1, SA-WA1/2020) in water and then wiped with a cleaning solution each day for five days.

Samples were collected by swabbing the sentinel cards pre-inoculation, post-inoculation, and post-wipe (Supplemental Fig. AB.1.S1).

For this study we used three viral loads: “high” (4 x 104), “medium” (1 x 104), and “low” (2.5 x 103) dilutions of SARS-CoV-2 viral genomic equivalents, as measured by droplet digital PCR. These concentrations were chosen to bracket the ranges we typically observed in classrooms during SASEA [9]. We used two different transport media: SDS (0.5% w/v sodium dodecyl sulfate (SDS), Acros Organics, 230420025), which we have previously shown to yield superior results in SARS-CoV-2 molecular assays [11], and VTM (Viral Transport Medium, NEST Scientific USA, 202016), which the FDA has approved for transporting SARS-CoV-2 samples that will be used for molecular or antigen testing [12]. The recipe for VTM as recommended by the CDC is Hank’s Balanced Salt Solution with 2% fetal bovine serum (FBS), 100µg/mL gentamicin, and 0.5 µg/mL amphotericin B [13]. We chose to use SDS at a concentration of 0.5% because it has already been shown to effectively inactivate SARS-CoV-2 after 30 minutes of contact time [14,15]. However, local public health laboratories performing SARS-CoV-2 monitoring on a larger scale, such as the San Diego County Public Health Laboratory, currently employ VTM for sample collection.

We tested three cleaning methods: benzalkonium chloride (BZK) antiseptic towelettes (Dynarex, 1331), Wet Wipe towelettes (Royal, RF1MB), and paper towels moistened with RNase Away (ThermoFisher Scientific, 10328011). BZK wipes contain 0.13% benzalkonium chloride, which is an antiseptic and a quaternary ammonium compound; Wet Wipes contain 1% bleach (sodium hypochlorite). Both BZK and sodium hypochlorite are effective at inactivating SARS-CoV-2, as well as other viruses, at

relevant concentrations [16-19], and are feasible to implement in school settings due to their cost and packaging (pre-packaged wipes are easy to distribute). RNase Away is a dilution of sodium hydroxide and was included because it is recommended by the FDA to minimize nucleic acid contamination [20,21]. However, it only serves as a positive control since it would not be practical for use in schools.

To continue benchmarking proven environmental pipelines [7, 9, 11] and to account for potential interactions, we used a factorial study design covering two swabbing media (SDS, VTM), three cleaning solutions (BZK wipes, Wet Wipes, RNase Away), and three viral spike-in concentrations (High, Medium, Low). Each condition was performed in triplicate for a total of 54 cards. A three-step swabbing process was performed on each card over a five-day period (Supplemental Fig. AB.1.S1). First, we swabbed each card at the start of the day (Step 1). Next, the viral spike-in was added to the card and a second swab was collected (Step 2). Lastly, the card was wiped with the cleaning solution and a final swab was collected (Step 3). Extraction and RT-qPCR were performed as described in our previous work, with VTM samples processed by the Perkin-Elmer pipeline and SDS samples processed by the Thermo pipeline described in that work [11].

2.3. Results

Our results demonstrated that all of the cleaning methods worked well at low viral load over 5 cleaning cycles, although cleaning failures were more frequent with BZK (Fig. 2.1). Both Wet Wipes and BZK performed well with SDS at medium viral loads, but only Wet Wipes performed well with VTM under these conditions. As expected from our past

work [11], SDS returned lower Cq values (better signal) than VTM on the same samples. Repeat cleaning did not degrade the sentinel card surface or the ability to detect signal.

Figure 2.1. Effect of cleaning solution at high, medium and low viral load with different swabbing media. On each day, three samples were taken: (1) before addition of viral particles, (2) after addition, and (3) after cleaning. Therefore, the expected pattern is a train of 5 spikes, starting at zero, rising to the maximum Cq value, returning to zero the same day, and staying at zero until the next day, as seen for SDS in the low load condition with RNase Away (bottom right panel, solid lines). High, medium, and low viral load were defined as (4×10^4), (1×10^4), and (2.5×10^3), respectively. Average Cq (Avg. Cq) was calculated as a mean Cq value from three samples. Two viral transport media were tested: SDS (0.5% w/v sodium dodecyl sulfate (SDS) and VTM (Viral Transport Medium). Effective cleaning reset Cq for each day. RNase Away was shown to be effective at each viral load, whereas benzalkonium chloride (BZK) and Wet Wipes were only effective at medium and low viral load.

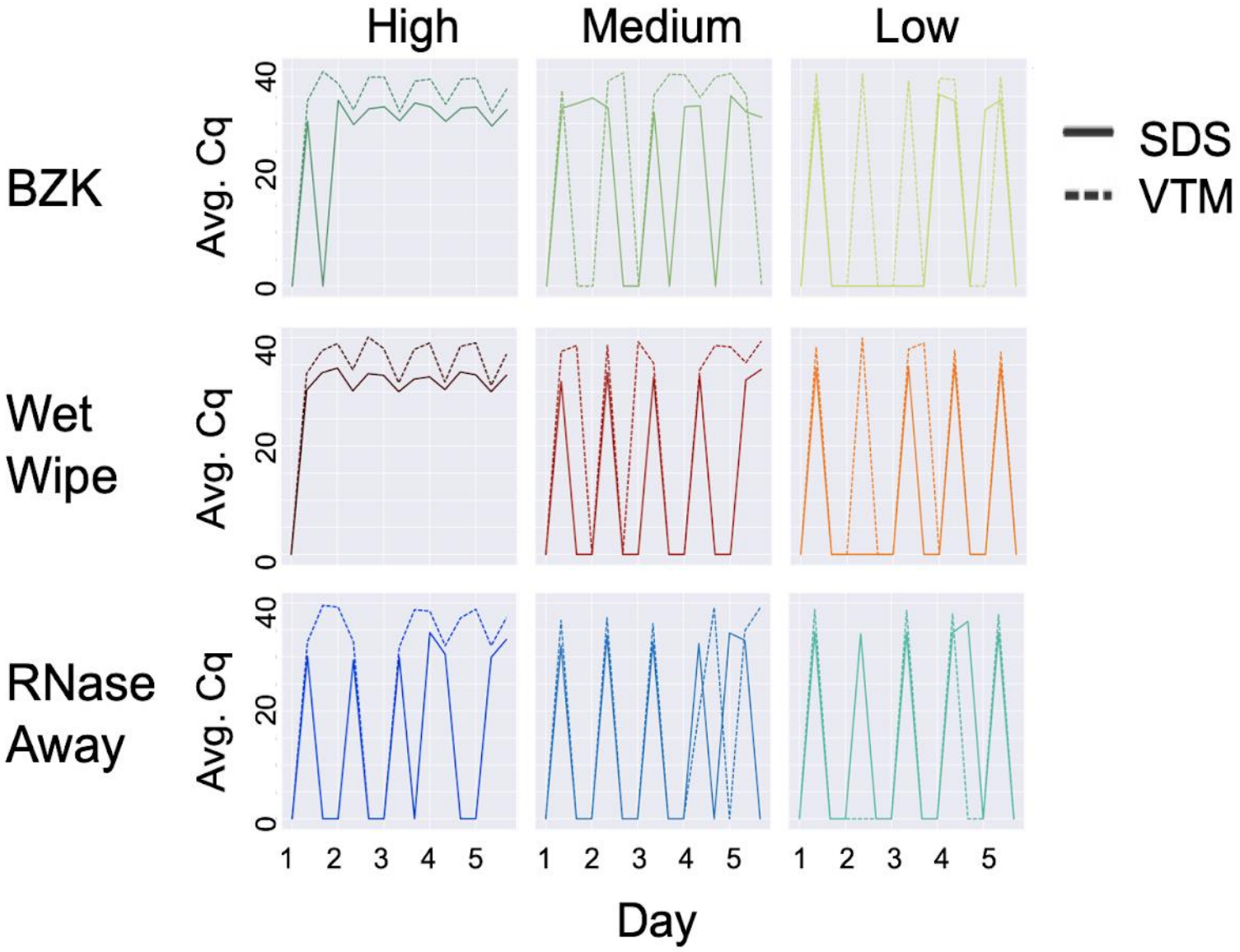
High
Medium
Low
BZK
Wet Wipe
RNase Away
Avg. Cq
0
20
40
1 2 3 4 5
Day
SDS
VTM

The difference in performance between the SDS and VTM conditions in terms of resetting signal can be explained by the properties of the swabbing media themselves. SDS is a surfactant meaning it has both a hydrophilic end, which is attracted to water, and a hydrophobic end that is attracted to the lipids making up the SARS-CoV-2 membrane. This allows SDS to disrupt the lipid membrane while at the same time making biomolecules more readily removable from the cards [22]. In contrast, the organic matter from the FBS in VTM introduces organic materials which act as viral clumping protective factors and can affect the efficacy of disinfecting agents with regard to inactivating viruses [18]. We indeed noticed that swabbing with VTM resulted in a leftover residue on the cards that was more difficult to wipe off regardless of the cleaning solution. The process of cleaning the card is reliant on removing organic material impurities and the BZK wipes are less efficient at this than the Wet Wipes. This poor performance of BZK with dried virus can be understood from a thermodynamic perspective. BZK is a cationic surfactant (positively charged) and will be attracted to the negatively charged virus and card surface. This means that BZK cannot effectively disperse the virus and so has relatively poor performance as a detergent [22]. When the swabbing media is VTM instead of SDS, this effect is amplified which is supported by a study aimed at understanding the result of adding 5% FBS to viral suspensions. FBS showed no influence on the virucidal capabilities of quaternary ammonium compounds except for BZK, decreasing the efficacy of BZK [23]. A second study provides possible further insight for the difference in performance between BZK and sodium hypochlorite. In this study, researchers examined the virucidal efficacy of BZK and sodium hypochlorite as measured by cell culture and the

genomic integrity of viruses after exposure to the two chemicals measured by RT-PCR. The study found that both compounds effectively inactivated SARS-CoV but that viral RNA could still be detected by PCR when BZK was used [19].

At high viral loads, only the combination of RNase Away and SDS was able to remove the signal. This was as expected since RNase Away is often used to ensure environments are RNA free for sensitive molecular assays [24,25]. Because the combination of RNase Away and SDS cannot be used at scale with existing infrastructure, we recommend sentinel card replacement at earliest convenience, rather than cleaning, if high viral loads (Cq < 30 with SDS or Cq < 35 with VTM) are detected on a sentinel card.

2.4. Discussion

An important consideration is the number of distinct genes recovered as matching in the RT-qPCR process, as this can make the difference between a sample being called as SARS-CoV-2 positive versus invalid. Because the peaks with the same viral load applied were highly reproducible across multiple days (reaching the same height in Fig. 2.1), for this analysis we could treat each day as a replicate of the pre-application, post-application, and post-cleaning sample conditions that were collected on each day. Fig. 2.2 shows the reproducibility of replicates with cleaning, including the number of genes amplified. Under low load conditions, as expected, cleaning was effective and non-zero values occurred nearly always post-application and disappeared on cleaning, with the exception of VTM samples which sometimes carried over (right hand column in Fig 2). In contrast, in the high load condition (left hand column in Fig. 2.2), cleaning was nearly

always ineffective except with RNase Away, not practical for classroom use. In the medium condition (middle column), all cleaning methods were effective with SDS but none were effective with VTM – the slightly higher cluster of Cq values are obtained with VTM in each case, consistent with expectations and with Fig. 2.1.

Figure 2.2. Cleaning solution efficiency after deliberate addition of viral load. Sampling was performed in three steps: initial virus amount (blank) was sampled from the wall for Step 1. Virus was deliberately loaded on the surface and sampled for Step 2. The surface was cleaned with different cleaning methods and sampled for qPCR analysis for Step 3. High, medium, and low viral load were defined as (4×10^4), (1×10^4), and (2.5×10^3), respectively. Average Cq (Avg. Cq) was calculated as a mean Cq value from three samples. Two viral transport media were tested: SDS (0.5% w/v sodium dodecyl sulfate (SDS) and VTM (Viral Transport Medium). Effective cleaning reset Cq for each day (steps 1 and 3), whereas ineffective cleaning retained high viral load (non-zero Cq) at these steps. The number of gene hits refers to how many gene targets were amplified during RT-qPCR across the triplicate samples: the qPCR method for the SDS samples targeted 3 genes for a total of 9 possible genes amplified while the method for the VTM samples targeted 2 genes for a total of 6 possible gene hits.

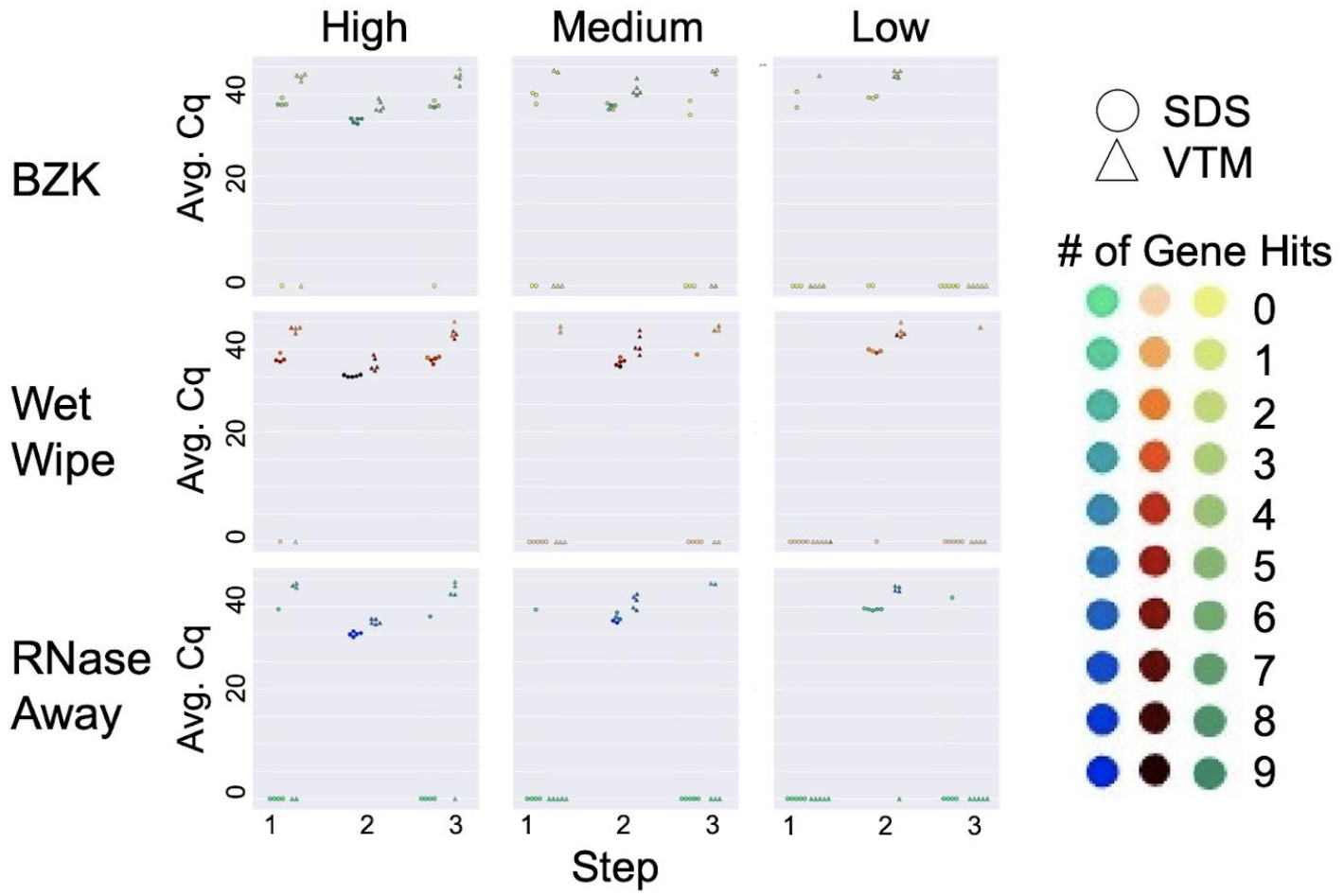
High
Medium
Low
BZK
Wet Wipe
RNase Away
Avg. Cq
0
20
40
1
2
3
Step
SDS
VTM
# of Gene Hits
0
1
2
3
4
5
6
7
8
9

Taken together, these results indicate that sentinel cards are an effective and practical solution for SARS-CoV-2 classroom monitoring, but that they must be cleaned carefully in order to remove carryover signal, and this process is easier with samples collected in SDS than in VTM (although cleaning with VTM is still possible). Because removing high viral load from sentinel cards is challenging, strong positives should be removed rather than cleaned. These findings are an important step to deployment of these cards at scale in projects such as SASEA.

2.5. Acknowledgements

This research was supported by NIH grant (K01MH112436) to R.F.M., the County of San Diego Health and Human Services Agency (Contract 563236), and the Career Award for Medical Scientists from the Burroughs Wellcome Fund to A.F.C. We thank Marisol Chacon, Evelyn S. Crescini, Bhavika Kapadia, Sydney C. Morgan, Alhakam Nouri, Christopher A. Ruiz, Phoebe Seaver, and Lizbeth Franco Vargas for their support with environmental SARS-CoV-2 detection as part of the EXCITE Lab.

The following reagent was deposited by the Centers for Disease Control and Prevention and obtained through BEI Resources, NIAID, NIH: SARS-Related Coronavirus 2, Isolate USA-WA1/2020, NR-52281.

Chapter 2, in full, is a reprint of the material as it appears in *mSystems*, “Sentinel Cards Provide Practical SARS-CoV-2 Monitoring in School Settings.” Cantú VJ, *et al*. The dissertation author was the primary investigator and first author of this paper.

2.6. References

1. Black E, Ferdig R, Thompson LA. 2021. K-12 Virtual Schooling, COVID-19, and Student Success. JAMA pediatrics 175:119–120.

2. van Lancker W, Parolin Z. 2020. COVID-19, school closures, and child poverty: a social crisis in the making. The Lancet Public Health 5:e243–e244.

3. White A, Liburd LC, Coronado F. 2021. Addressing Racial and Ethnic Disparities in COVID-19 Among School-Aged Children: Are We Doing Enough? Preventing chronic disease 18:1–11.

4. Rubin D, Coffin S, Fisher B, Gerber J, Matone M. 2022. Guidance for In-person Education in K-12 Educational Settings. Children's Hospital of Philadelphia.

5. Johnson KE, Stoddard M, Nolan RP, White DE, Hochberg NS, Chakravarty A. 2021. In the long shadow of our best intentions: Model-based assessment of the consequences of school reopening during the COVID-19 pandemic. PloS one 16.

6. Karthikeyan S, Nguyen A, McDonald D, Zong Y, Ronquillo N, Ren J, Zou J, Farmer S, Humphrey G, Henderson D, Javidi T, Messer K, Anderson C, Schooley R, Martin NK, Knight R. 2021. Rapid, Large-Scale Wastewater Surveillance and Automated Reporting System Enable Early Detection of Nearly 85% of COVID-19 Cases on a University Campus. mSystems 6.

7. Salido RA, Cantú VJ, Clark AE, Leibel SL, Foroughishafiei A, Saha A, Hakim A, Nouri A, Lastrella AL, Castro-Martínez A, Plascencia A, Kapadia BK, Xia B, Ruiz CA, Marotz CA, Maunder D, Lawrence ES, Smoot EW, Eisner E, Crescini ES, Kohn L, Franco Vargas L, Chacón M, Betty M, Machnicki M, Wu MY, Baer NA, Belda-Ferre P, de Hoff P, Seaver P, Ostrander RT, Tsai R, Sathe S, Aigner S, Morgan SC, Ngo TT, Barber T, Cheung W, Carlin AF, Yeo GW, Laurent LC, Fielding-Miller R, Knight R. 2021. Analysis of SARS-CoV-2 RNA Persistence across Indoor Surface Materials Reveals Best Practices for Environmental Monitoring Programs. mSystems 6.

8. Cantú VJ, Salido RA, Huang S, Rahman G, Tsai R, Valentine H, Magallanes CG, Aigner S, Baer NA, Barber T, Belda-Ferre P, Betty M, Bryant M, Casa-Maya M, Castro-Martínez, Chacón M, Cheung W, Crescini ES, de Hoff P, Eisner E, Farmer S, Hakim A, Kohn L, Lastrella AL, Lawrence ES, Morgan SC, Ngo TT, Nouri A, Plascencia A, Ruiz CA, Sathe S, Seaver P, Shwartz T, Smoot EW, Ostrander T, Valles T, Yeo GW, Laurent LC, Fielding-Miller R, Knight R. (2021). SARS-CoV-2 Distribution in Residential Housing Suggests Contact Deposition and Correlates with *Rothia* sp. (submitted for publication).

9. Fielding-Miller R, Karthikeyan S, Gaines T, Garfein RS, Salido R, Cantu V, Kohn L, Martin NK, Wijaya C, Flores M, Omaleki V, Majnoonian A, Gonzalez-Zuniga P,

Nguyen M, Vo A v, Le T, Duong D, Hassani A, Dahl A, Tweeten S, Jepsen K, Henson B, Hakim A, Birmingham A, Mark AM, Nasamran CA, Rosenthal SB, Moshiri N, Fisch KM, Humphrey G, Farmer S, Tubb HM, Valles T, Morris J, Kang J, Khaleghi B, Young C, Akel AD, Eilert S, Eno J, Curewitz K, Laurent LC, Rosing T, SEARCH, Knight R. 2021. Wastewater and surface monitoring to detect COVID-19 in elementary school settings: The Safer at School Early Alert project. medRxiv : the preprint server for health sciences https://doi.org/10.1101/2021.10.19.21265226

10. Renninger N, Nastasi N, Bope A, Cochran SJ, Haines SR, Balasubrahmaniam N, Stuart K, Bivins A, Bibby K, Hull NM, Dannemiller KC. 2021. Indoor Dust as a Matrix for Surveillance of COVID-19. mSystems 6.

11. Cantú VJ, Belda-Ferre P, Salido RA, Tsai R, Austin B, Jordan W, Asudani M, Walster A, Magallanes CG, Valentine H, Manjoonian A, Wijaya C, Omaleki V, Sanders K, Aigner S, Baer NA, Betty M, Castro-Martínez A, Chacón M, Cheung W, Crescini ES, de Hoff P, Eisner E, Hakim A, Kapadia B, Lastrella AL, Lawrence ES, Ngo TT, Ostrander T, Sathe S, Seaver P, Smoot EW, Carlin AF, Yeo GW, Laurent LC, Manlutac AL, Fielding-Miller R, Knight R. 2022. Implementation of Practical Surface SARS-CoV-2 Surveillance in School Settings (submitted for publication).

12. U.S. Department of Health and Human Services Food and Drug Administration. 2021. Enforcement Policy for Viral Transport Media During the Coronavirus Disease 2019 (COVID-19) Public Health Emergency (Revised). Available at: https://www.fda.gov/regulatory-information/search-fda-guidance-documents/enforcement-policy-viral-transport-media-during-coronavirus-disease-2019-covid-19-public-health. (Accessed: 12 March 2022)

13. Centers for Disease Control and Prevention. Preparation of Viral Transport Medium. 2020. Available at: https://www.cdc.gov/coronavirus/2019-ncov/downloads/Viral-Transport-Medium.pdf. (Accessed: 12 March 2022)

14. Patterson EI, Prince T, Anderson ER, Casas-Sanchez A, Smith SL, Cansado-Utrilla C, Solomon T, Griffiths MJ, Acosta-Serrano Á, Turtle L, Hughes GL. 2020. Methods of Inactivation of SARS-CoV-2 for Downstream Biological Assays. J Infect Dis 222:1462–1467.

15. Welch SR, Davies KA, Buczkowski H, Hettiarachchi N, Green N, Arnold U, Jones M, Hannah MJ, Evans R, Burton C, Burton JE, Guiver M, Cane PA, Woodford N, Bruce CB, Roberts ADG, Killip MJ. 2020. Analysis of inactivation of SARS-CoV-2 by specimen transport media, nucleic acid extraction reagents, detergents, and fixatives. J Clin Microbiol 58.

16. Ogilvie BH, Solis-Leal A, Lopez JB, Poole BD, Robison RA, Berges BK. 2021. Alcohol-free hand sanitizer and other quaternary ammonium disinfectants quickly and effectively inactivate SARS-CoV-2. J Hosp Infect 108:142–145.

17. Kwok CS, Dashti M, Tafuro J, Nasiri M, Muntean EA, Wong N, Kemp T, Hills G, Mallen CD. 2021. Methods to disinfect and decontaminate SARS-CoV-2: a systematic review of in vitro studies. Ther Adv Infect Dis 8.

18. Lin Q, Lim JYC, Xue K, Yin P, Yew M, Owh C, Chee PL, Loh XJ. 2020. Sanitizing agents for virus inactivation and disinfection. View 1:e16.

19. Ansaldi F, Banfi F, Morelli P, Valle L, Durando P, Sticchi L, Contos S, Gasparini R, Crovari P. 2004. SARS-CoV, influenza A and syncitial respiratory virus resistance against common disinfectants and ultraviolet irradiation. J Prev Med Hyg 45:5–8.

20. U.S. Food and Drug Administration. 2021. CovidNow SARS-CoV-2 Assay – Letter of Authorization. Available at: https://www.fda.gov/media/153172/download. (Accessed: 12 March 2022)

21. Lighthouse Lab Services. 2021. CovidNow SARS-CoV-2 Assay - Instructions for Use. Available at: https://www.lighthouselabservices.com/wp-content/uploads/2021/10/IFU-CovidNow-20211012-FINAL-CLEAN.pdf. (Accessed: 12 March 2022)

22. Simon M, Veit M, Osterrieder K, Gradzielski M. 2021. Surfactants – Compounds for inactivation of SARS-CoV-2 and other enveloped viruses. Curr Opin Colloid Interface Sci 55:101479.

23. Tsujimura K, Murase H, Bannai H, Nemoto M, Yamanaka T, Kondo T. 2015. Efficacy of five commercial disinfectants and one anionic surfactant against equine herpesvirus type 1. J Vet Med Sci 77:1545–1548

24. Quigley MF, Almeida JR, Price DA, Douek DC. 2011. Unbiased molecular analysis of T cell receptor expression using template-switch anchored RT-PCR. Curr Protoc Immunol CHAPTER:Unit10.33.

25. Sessitsch A, Gyamfi S, Stralis-Pavese N, Weilharter A, Pfeifer U. 2002. RNA isolation from soil for bacterial community and functional analysis: evaluation of different extraction and soil conservation protocols. J Microbiol Methods 51:171–179.

Chapter 3. Implementation of Practical Surface SARS-CoV-2 Surveillance in School Settings

Abstract

Surface sampling for SARS-CoV-2 RNA detection has shown considerable promise to detect exposure of built environments to infected individuals shedding virus who would not otherwise be detected. Here we compare two popular sampling media (VTM and SDS) and two popular workflows (Thermo and PerkinElmer) for implementation of a surface sampling program suitable for environmental monitoring in public schools. We find that the SDS/Thermo pipeline shows superior sensitivity and specificity, but that the VTM/PerkinElmer pipeline is still sufficient to support surface surveillance in any indoor setting with stable cohorts of occupants (e.g., schools, prisons, group homes, etc.) and may be used to leverage existing investments in infrastructure.

Importance

The ongoing COVID-19 pandemic has claimed the lives of over 5 million people worldwide. Due to high density occupancy of indoor spaces for prolonged periods of time, schools are often of concern for transmission, leading to widespread school closings to combat pandemic spread when cases rise. Since pediatric clinical testing is expensive and difficult from a consent perspective, we have deployed in SASEA (Safer At School Early Alert) surface sampling, which allows for detection of SARS-CoV-2 from surfaces within a classroom. In this previous work, we developed a high throughput method which

requires robotic automation and specific reagents that are often not available for public health laboratories such as the San Diego County Public Health Laboratory (SDPHL). Therefore, we benchmarked our method (Thermo pipeline) against SDPHL's (PerkinElmer) more widely used method for the detection and prediction of SARS-CoV-2 exposure. While our method shows superior sensitivity (false negative rate of 9% vs 27% for SDPHL), the SDPHL pipeline is sufficient to support surface surveillance in indoor settings. These findings are important since they show that existing investments in infrastructure can be leveraged to slow the spread of SARS-CoV-2 not in just the classroom but also in prisons, nursing homes, and other high-risk, indoor settings.

3.1. Introduction

Over the past two years, the COVID-19 pandemic has claimed the lives of over 5 million people worldwide [1]. Due to high density occupancy of indoor spaces for prolonged periods of time, schools are often of concern for transmission, leading to widespread school closings to combat pandemic spread when cases rise. However, K-12 schools are important resources for communities, which, besides education and childcare, often provide food, authoritative and trusted information, and a sense of belonging and security [2, 3]. Therefore, alternative approaches that keep children in school are highly desirable. Performing pediatric clinical testing, such as SARS-CoV-2 detection via RT-qPCR, is expensive, difficult from a consent perspective, and increasingly politicized. Wastewater testing, although highly effective even at the level of individual cases and buildings [4], can only identify SARS-CoV-2 among the subset of individuals that defecate at school, and often cannot provide spatial resolution at finer

levels. A complementary method that we have deployed in Safer At School Early Alert (SASEA) [5] is surface sampling, which allows detection of SARS-CoV-2 from surfaces within a classroom. This is a screening method, not a diagnostic; however, even without high sensitivity, surface sampling provides visibility into environments where individuals will not consent to testing and where cases are not picked up through wastewater. In particular, surface sampling can localize cases within a single classroom [5].

In previous work, we showed SARS-CoV-2 persists on a range of school-relevant surfaces using our SASEA workflow, based on collecting swabs into a 0.5% sodium dodecyl sulfate (SDS) w/v solution (Acros Organics, 230420025), performing nucleic acid extraction on the Kingfisher Flex liquid-handling robot (Thermo Scientific), and performing RT-qPCR using the QuantStudio 7 [5]. We implemented this protocol in the research phase of SASEA [3, 6]. However, this protocol requires specialized reagents and equipment that is not generally available to public health laboratories, and we needed to test its generality using workflows already operational in the San Diego County Public Health Laboratory (SDPHL), which employs Viral Transport Medium (VTM) (NEST Scientific USA, 202016) for sample collection, and the PerkinElmer (PE) workflow for nucleic acid extraction and RT-qPCR (Supplementary Table S2) [7]. Adapting surface sampling to this widely used clinical workflow would enable its application to an entirely new sampling modality and allow surface sampling to be incorporated into a wide range of programs in schools, prisons, nursing homes, and other high-risk, indoor settings.

3.2. Results

To assess whether conclusions drawn from our established Thermo pipeline [6] could be generalized to the more widespread PerkinElmer pipeline, we first compared the performance of both methods using contrived samples. Briefly, the Thermo pipeline collects surface swabs into Matrix tubes containing 0.5% w/v SDS in water, extracts nucleic acids using the Omega MagBind Viral RNA/DNA kit (SKU: M6246-03) using the KingFisher Flex platform, and detects SARS-CoV-2 presence through a miniaturized 3µL-reaction version of the TaqPath™ COVID-19 Combo Kit (ThermoFisher Scientific, A47814) on a QuantStudio 7 Pro qPCR machine (Thermo Fisher Scientific). The PerkinElmer pipeline follows the Emergency Use Authorization of sample collection into Viral Transport Media, requires a heat-inactivation step (65C for 15 mins), extracts nucleic acids using the chemagic 360 platform and reagents, and detects SARS-CoV-2 presence using the standard 15 µL-reaction protocol of the PerkinElmer New Coronavirus Nucleic Acid Detection Kit on an Analytik Jena qTOWER3 84 G Real-Time PCR system.

To manufacture the contrived samples, we deposited 10 µL of a heat-inactivated SARS-CoV-2 dilution series (strain WA-1, SA-WA1/2020) on laminated cards, making triplicate cards for each of the three concentrations used (206, 1024, 4096 GEs/µL). Nine replicates were swabbed with 0.5% SDS and processed by the Thermo pipeline while the other nine were swabbed with VTM and processed by the PerkinElmer pipeline. We found that the two platforms yielded highly correlated results (Pearson correlation, $r = 0.810$, $p = 2.87 \times 10\text{-}6$) but the SDS/Thermo pipeline was more sensitive by ~4 Cq units on average (Fig. 3.1).

Figure 3.1. Comparison of SDS/Thermo and VTM/PE pipelines on contrived samples. Average Cq values of contrived samples with the SDS/Thermo pipeline versus the Average Cq of matched samples processed through VTM/PerkinElmer pipeline. A linear regression was overlaid on the measured data (in blue) (Pearson correlation, m = 1.16, b = -1.14, r = 0.81, p = 2.87 x 10-6). The gray line represents the expected Cq values where x = y, i.e., if the two assays performed identically on the same samples.

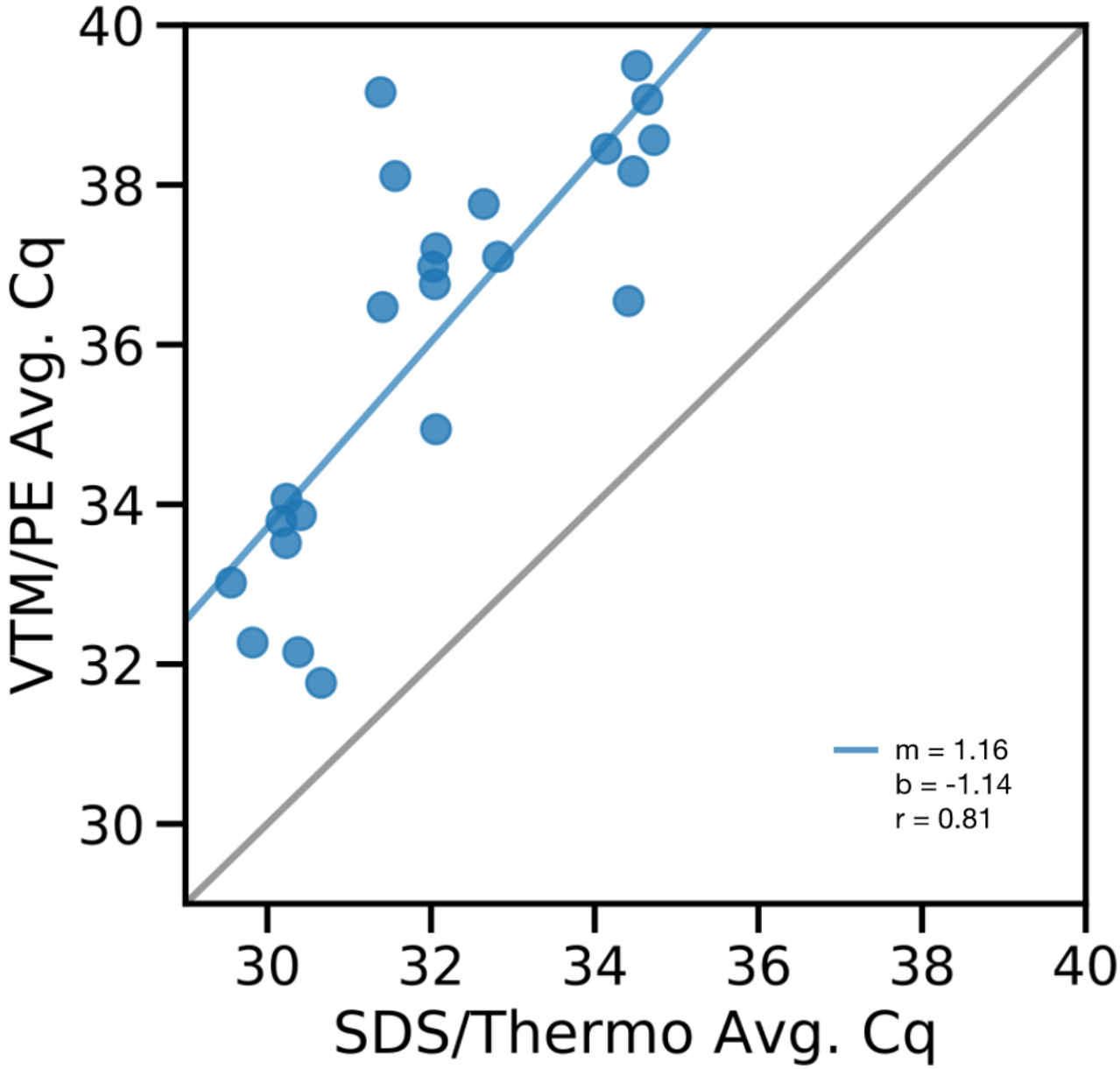
VTM/PE Avg. Cq
SDS/Thermo Avg. Cq
40
38
36
34
32
30
30
32
34
36
38
40
m = 1.16
b = -1.14
r = 0.81

To test whether these conclusions extended to a real-world setting, we collected duplicate biological replicates of 30 samples from isolation housing in which known COVID-19 patients, confirmed by positive anterior nares RT-qPCR, were housed (IRB-approved research under HRPP UCSD protocol 200477). The distribution of sampled surfaces is given in Table 3.1, and their spatial localization in one of the apartments is given in Fig. 3.2 as an example. In a crossover protocol to separate the effects of the swabbing/transport medium and RNA extraction from the effects of the qPCR assay, we ran each protocol through RNA extraction, exchanged RNA between the UCSD lab and the SDPHL, then subjected the resulting RNA to RT-qPCR on the other platform (Supplementary Table S1). This created four sets of samples summarized in Supplementary Table S3.

Table 3.1. Number of detection events per feature per apartment. The text within each cell indicates the material of the sampled feature and the heatmap coloring represents the counts of positive detection events from the different combinations of extraction and RT-qPCR facility. A value of 4 indicates detection in all 4 pipeline permutations, whereas 0 indicates no detection in any of the combinations.

Room Type	Feature	Apt A	Apt B	Apt C
Bathroom	bathroom sink	porcelain	porcelain	porcelain
	bathroom door handle		stainless steel	
	toilet floor	ceramic	ceramic	ceramic
Bedroom	bed headboard	sealed wood	raw wood	sealed wood
	bedside floor	carpet	vinyl	carpet
	bedside table	sealed wood	wicker	sealed wood
Kitchen	kitchen counter		laminate	laminate
	kitchen sink handles	stainless steel	stainless steel	stainless steel
	kitchen table	laminate		laminate
Living Room	desk top	sealed wood		sealed wood
	coffee table		sealed wood	
	desk chair	fabric		
	light switch	plastic	plastic	plastic

Figure 3.2. Ili mapping of positive detection events across pipeline combinations on a representative 3D render of the rooms swabbed. This 3D rendering represents the relationship between rooms and features that were swabbed in Apt C (Table 1). The color scale represents the number of positive detection events returned across the combinations of extraction and RT-qPCR facilities.


4
3
2
1
0

We found that each laboratory performed best when sample extraction and RT-qPCR processing occurred in the same facility, presumably because of RNA degradation during transit (Fig. 3.3A-3.3B). A Kruskal-Wallis H test confirmed that the mean Cq's differ significantly across the pipeline combinations ($H = 26.9$, $p = 6.22 \times 10\text{-}6$) (Fig 3C). Pairwise Mann-Whitney U tests between the groups showed that the Cq ranks are significantly different between groups processed at the different PCR facilities, but there is no significant difference for groups within PCR facility. The SDPHL RT-qPCR assay performed better on the samples processed with the PE pipeline than on the Thermo/PE paired samples (mean Cq difference 0.88, $U = 0.693$, $p > 0.1$), whereas the UCSD RT-qPCR assay performed better with the samples processed with the Thermo pipeline than with the paired PE/Thermo samples (mean Cq difference 1.2, $U = 1.48$, $p > 0.1$). However, the Thermo workflow provided an advantage in sensitivity of 5.1 Cq units on average over the PE workflow yielding a p-value of $5.86 \times 10\text{-}3$ after correcting for multiple comparisons (FDR-Benjamin/Hochberg) ($U = 3.72$) . None of the assays were perfect: the Thermo pipeline detected 6 samples that the PE pipeline counted as negative, and the PE pipeline detected 2 samples that the Thermo pipeline counted as negative (Supplementary Table S1). To calculate the sensitivity of each pipeline, we assumed that if at least one of the pipeline combinations (Thermo, Thermo/PE, PE, PE/Thermo) detected the presence of virus, then that sample could be considered a true positive resulting in a true positivity rate of 91% for the Thermo pipeline and 73% for the PE pipeline. However, we were unable to make any assumptions about the true negative rate and are unable to calculate the specificity of each pipeline.

Figure 3.3. Comparison of SDS/Thermo and VTM/PE pipeline combinations on real samples. A&B) Scatterplots showing the performance of the Thermo (UCSD) and PerkinElmer (PHL) RT-qPCR workflows on surface samples extracted at both facilities. Empty x's and o's next to the sample name indicates that no viral signal was detected in that sample for that combination of extraction and RT-qPCR facility. C) Swarmplots showing that the sensitivity of the Thermo RT-qPCR workflow is higher than that of the PE pipeline (Kruskal-Wallis, $p < 0.01$). Post hoc analysis showed that there was no significant difference between samples that underwent RT-qPCR at the same facility ($p > 0.1$) but there were differences between RT-qPCR facilities ($p < 0.05$). D) Venn diagram showing the number of positive samples detected by each of the extraction facility/RT-qPCR pipeline combinations.

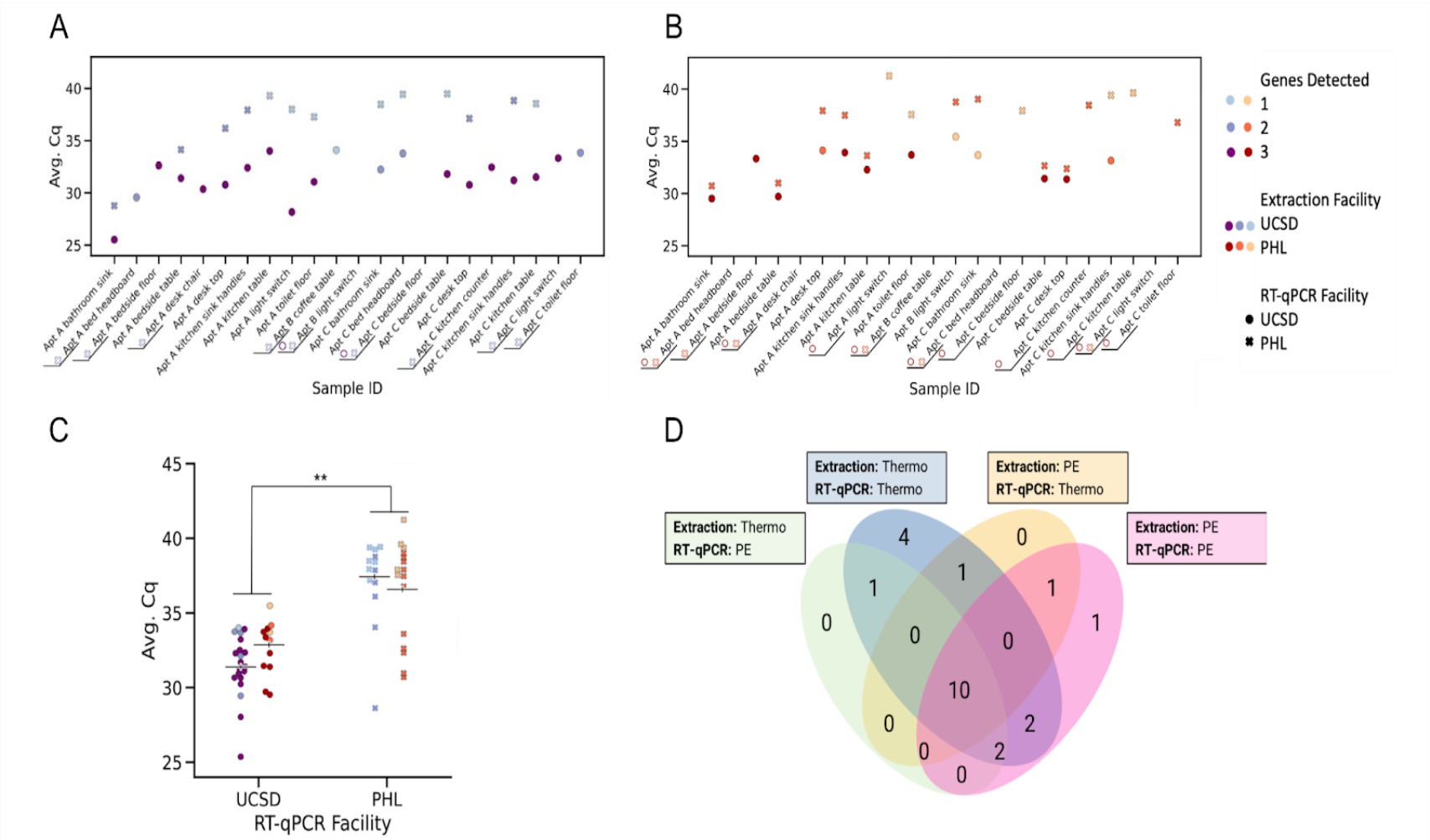
A
B
Avg. Cq
Sample ID
Genes Detected
1
2
3
Extraction Facility
UCSD
PHL
RT-qPCR Facility
UCSD
PHL
C
Avg. Cq
RT-qPCR Facility
UCSD
PHL
**
D
Extraction: Thermo
RT-qPCR: Thermo
Extraction: PE
RT-qPCR: Thermo
Extraction: Thermo
RT-qPCR: PE
Extraction: PE
RT-qPCR: PE

3.3. Discussion

We note that although the PE assay is less sensitive, but this level of accuracy is sufficient for projects such as SASEA, where the goal is to screen environments for further resource allocation for COVID-19 mitigation efforts rather than to perform a diagnostic test. In conclusion, we note that although the optimized Thermo protocol we developed for SASEA offers considerable sensitivity advantages, the PE assay is still pragmatically useful for classroom SARS-CoV-2 surveillance and can leverage large existing investments in infrastructure and expertise.

3.4. Materials and Methods

Surface sampling with two transport media (VTM and SDS) and subsequent nucleic extraction and SARS-CoV-2 readout with two RT-qPCR pipelines (Thermo and PerkinElmer) are compared in a factorial design.

UCSD protocol:

Nucleic acid extraction:

Individual 96-well tube racks were vortexed for 5 minutes at 3200 RPM to promote the suspension of viral particles from the swabs into the 0.5% w/v SDS solution. Afterwards, 150 µL of the suspension buffer (0.5% SDS) were transferred with a multichannel pipette into barcoded deep well extraction plates (ThermoFisher Scientific, 95040450) and processed using the Omega MagBind Viral DNA/RNA kit (Omega Bio-Tek, M6246) on the Kingfisher Flex (ThermoFisher Scientific) platform following manufacturer's protocol with the following modifications: only 150µL of sample input was used (instead of the recommended 200µL) and 10 µL of MS2 phage was added to each well as an extraction control.

RT-qPCR (Multiplexed TaqPath)

Viral gene detection assays were performed using the RT-qPCR-based TaqPath™ COVID-19 Combo Kit (ThermoFisher Scientific, A47814) on a QuantStudio 7 Pro with a 384-well sample block (ThermoFisher Scientific, A43185) according to the manufacturer's protocol with the following modifications: 2 µL of purified RNA was added to a 1 µL reaction mix containing 0.75 µL TaqPath 4x

Enzyme mix (ThermoFisher Scientific, A28523), 0.15 µL multiplex probe mix, and 0.1 µL nuclease free water, for a total reaction volume of 3 µL. Low volume transfers (< 5µL) were done with Mosquito HV Liquid Handlers (SPT Labtech). The following RT-qPCR cycling conditions were used: 25°C for 2 minutes, 53°C for 10 minutes, 95°C for 2 minutes, 55 cycles of 95°C for 3 seconds, and 60°C for 30 seconds. The signal was measured at the end of each 30 second interval at 60°C. Baseline determination and quantification cycle (Cq) signal determination were made using the Design and Analysis v2.4.3 software (Applied Biosystems) using the relative threshold (Crt) method. Positive calls for individual gene reporters were made according to Table S3.

SDPHL protocol:

<u>Nucleic acid extraction:</u>

Environmental samples in VTM were heat-inactivated in a bead-bath at 65C for 15 minutes, then cooled at 2-8C for a minimum of 10 minutes prior to processing. Assay controls (positive, negative, and internal controls) were thawed prior to use. Additional reagents (Poly A RNA and Proteinase K) were prepared per kit instructions prior to use. Specimens were brought to room temperature, placed into sample racks, and loaded onto the Janus Reformatter Robot. From the Janus Reformatter, samples and their corresponding reagent plates were transferred to the Chemagic 360 instrument for extraction by the manufacturer's protocol.

RT-qPCR:

Extract plates from the Chemagic 360 were transferred to the Janus qPCR Workstation Robot, along with qPCR master mix reagents, and loaded into a 384-qPCR plate. Viral gene detection assays were performed using the RT-qPCR-based PerkinElmer® New Coronavirus Nucleic Acid Detection Kit (2019-nCOV-PCR-AUS) on an Analytik Jena qTOWER^3 84 G Real-Time PCR system with a 384-well sample block according to the manufacturer's protocol for 15ul reaction. The following RT-qPCR cycling conditions were used: 37C 2 min.; 50C 5 min.; 42C 35 min.; 94C 10 min.; 45 cycles of 94C 10 sec., 55C 15 sec.; 65C 45 sec. The .trf method file generated by the Janus qPCR Workstation Robot was copied and transferred to the Analytic Jena as the qPCR method. Results were analyzed following assay processing. Interpretation of results was performed using qPCRSoft 384 for the Analytik Jena.

Fluorophore probes used for detection of two COVID targets (N [nucleocapsid] gene and ORF1ab [open reading frame 1 ab]) were FAM and Rox respectively. The IC (bacteriophage MS2) used a Hex fluorophore probe. Thresholds used for interpretation were between 5 and 15 dRn (delta in normalized reporting value). If a sample had either COVID target detected with Ct values below 42 at a threshold of 15, the sample was determined positive. Samples with detectable Internal Control but without detectable values for either of the two COVID targets were reported as negative. Samples which only had COVID targets within 'detectable' range at a threshold of 5 but outside of 'detectable' range at threshold of 15 (Ct above 42) were considered inconclusive; these were treated as

'negative' for reporting. Samples without positive values for either of the two COVID targets in addition to failed Internal Controls were considered invalid, and reported as such.

3.5. Acknowledgements

This research was supported by NIH grant (K01MH112436) to RFM, the County of San Diego Health and Human Services Agency (Contract 563236), and the Career Award for Medical Scientists from the Burroughs Wellcome Fund to A.F.C. We thank Marisol Chacon, Sydney C. Morgan, Alhakam Nouri, Ashley Plascencia, Christopher A. Ruiz, and Lizbeth Franco Vargas for their support with environmental SARS-CoV-2 detection as part of the EXCITE Lab.

The following reagent was deposited by the Centers for Disease Control and Prevention and obtained through BEI Resources, NIAID, NIH: SARS-Related Coronavirus 2, Isolate USA-WA1/2020, NR-52281.

Chapter 3, in full, is a reprint of the material as it appears in *mSystems*, "Implementation of Practical Surface SARS-CoV-2 Surveillance in School Settings. " Cantú VJ, Sanders K, *et al*. The dissertation author was the primary investigator and first author of this paper.

3.6. References

1. WHO Coronavirus (COVID-19) Dashboard | WHO Coronavirus (COVID-19) Dashboard With Vaccination Data. Available at: https://covid19.who.int/. (Accessed: 20th November 2021)

2. Guidance for COVID-19 Prevention in K-12 Schools | CDC. Available at: https://www.cdc.gov/coronavirus/2019-ncov/community/schools-childcare/k-12-guidance.html#anchor_1625662107144. (Accessed: 20th November 2021)

3. Fielding-Miller R, Karthikeyan S, Gaines T, Garfein RS, Salido R, Cantu V, Kohn L, Martin NK, Wijaya C, Flores M, Omaleki V, Majnoonian A, Gonzalez-Zuniga P, Nguyen M, Vo A v, Le T, Duong D, Hassani A, Dahl A, Tweeten S, Jepsen K, Henson B, Hakim A, Birmingham A, Mark AM, Nasamran CA, Rosenthal SB, Moshiri N, Fisch KM, Humphrey G, Farmer S, Tubb HM, Valles T, Morris J, Kang J, Khaleghi B, Young C, Akel AD, Eilert S, Eno J, Curewitz K, Laurent LC, Rosing T, SEARCH, Knight R. 2021. Wastewater and surface monitoring to detect COVID-19 in elementary school settings: The Safer at School Early Alert project. medRxiv : the preprint server for health sciences https://doi.org/10.1101/2021.10.19.21265226.

4. Kalluri N, Kelly C, Garg A. 2021. Child Care During the COVID-19 Pandemic: A Bad Situation Made Worse. Pediatrics 147.

5. Karthikeyan S, Nguyen A, McDonald D, Zong Y, Ronquillo N, Ren J, Zou J, Farmer S, Humphrey G, Henderson D, Javidi T, Messer K, Anderson C, Schooley R, Martin NK, Knight R. 2021. Rapid, Large-Scale Wastewater Surveillance and Automated Reporting System Enable Early Detection of Nearly 85% of COVID-19 Cases on a University Campus. mSystems 6.

6. Salido RA, Cantú VJ, Clark AE, Leibel SL, Foroughishafiei A, Saha A, Hakim A, Nouri A, Lastrella AL, Castro-Martínez A, Plascencia A, Kapadia BK, Xia B, Ruiz CA, Marotz CA, Maunder D, Lawrence ES, Smoot EW, Eisner E, Crescini ES, Kohn L, Franco Vargas L, Chacón M, Betty M, Machnicki M, Wu MY, Baer NA, Belda-Ferre P, de Hoff P, Seaver P, Ostrander RT, Tsai R, Sathe S, Aigner S, Morgan SC, Ngo TT, Barber T, Cheung W, Carlin AF, Yeo GW, Laurent LC, Fielding-Miller R, Knight R. 2021. Analysis of SARS-CoV-2 RNA Persistence across Indoor Surface Materials Reveals Best Practices for Environmental Monitoring Programs. mSystems 6.

7. PerkinElmer. Instructions for PerkinElmer New Coronavirus Nucleic Acid Detection Kit, v 10.0. https://www.fda.gov/media/136410/download (2021).

Chapter 4. SARS-CoV-2 Distribution in Residential Housing Suggests Contact Deposition and Correlates with Rothia sp.

Abstract

Monitoring severe acute respiratory syndrome coronavirus 2 (SARS-CoV-2) on surfaces is emerging as an important tool for identifying past exposure to individuals shedding viral RNA. Our past work has demonstrated that SARS-CoV-2 reverse transcription-quantitative PCR (RT-qPCR) signals from surfaces can identify when infected individuals have touched surfaces such as Halloween candy, and when they have been present in hospital rooms or schools. However, the sensitivity and specificity of surface sampling as a method for detecting the presence of a SARS-CoV-2 positive individual, as well as guidance about where to sample, has not been established. To address these questions, and to test whether our past observations linking SARS-CoV-2 abundance to *Rothia* sp. in hospitals also hold in a residential setting, we performed detailed spatial sampling of three isolation housing units, assessing each sample for SARS-CoV-2 abundance by RT-qPCR, linking the results to 16S rRNA gene amplicon sequences (to assess the bacterial community at each location) and to the Cq value of the contemporaneous clinical test. Our results show that the highest SARS-CoV-2 load in this setting is on touched surfaces such as light switches and faucets, but detectable signal is present in many non-touched surfaces (e.g., floors) that may be more relevant in settings such as schools where mask wearing is enforced. As in past studies, the bacterial community predicts which samples are positive for SARS-CoV-2, with *Rothia* sp. showing a positive association.

Importance

Surface sampling for detecting SARS-CoV-2, the virus that causes coronavirus disease 2019 (COVID-19), is increasingly being used to locate infected individuals. We tested which indoor surfaces had high versus low viral loads by collecting 381 samples from three residential units where infected individuals resided, and interpreted the results in terms of whether SARS-CoV-2 was likely transmitted directly (e.g. touching a light switch) or indirectly (e.g. by droplets or aerosols settling). We found highest loads where the subject touched the surface directly, although enough virus was detected on indirectly contacted surfaces to make such locations useful for sampling (e.g., in schools, where students do not touch the light switches and also wear masks so they have no opportunity to touch their face and then the object). We also documented links between the bacteria present in a sample and the SARS-CoV-2 virus, consistent with earlier studies.

4.1 Introduction

Environmental monitoring for severe acute respiratory syndrome coronavirus 2 (SARS-CoV-2) RNA by reverse transcription-quantitative polymerase chain reaction (RT-qPCR) is increasingly gaining acceptance. In the Safer at School Early Alert (SASEA) (https://saseasystem.org/) project, daily surface swabbing was employed as part of an effort to detect coronavirus disease 2019 (COVID-19) cases in nine elementary schools. This study identified 89 clinically positive COVID-19 cases, 33% preceded by a room-matched surface positive (1). As pandemic response measures like SASEA become more widely implemented, understanding where SARS-CoV-2 signatures will most likely be

found reduces cost and labor of surface swabbing in large facilities. Previous work has focused on sampling arbitrary surfaces in isolation and congregate care facilities, homes, and hospitals, with varying detection performance obscuring which surfaces are best for monitoring COVID-19 spread (2-6). Counterintuitively, high-touch hospital surfaces expected to accumulate viral load, including door handles and patient bed rails, can yield *lower* SARS-CoV-2 detection rates, presumably because they are cleaned more often (7-8).

Most microbes in the built environment come from human inhabitants (9-11). Oral, gut, and skin microbiomes of COVID-19 patients change during disease (8,12-13); therefore, SARS-CoV-2 positive built environmental samples may differ in *bacterial* communities from SARS-CoV-2 negative samples. This has been documented in a hospital setting, with associations between SARS-CoV-2 status (Detected/Not Detected) and both the overall microbial community and *Rothia* spp. specifically (8).

To extend these results to a residential setting and understand how SARS-CoV-2 is distributed in the living space of an infected individual, we performed environmental sampling in the apartments of three people who recently tested positive for COVID-19 (Sup. Fig. AD.1.S1) while quarantined in an isolation facility. On the day of swabbing, each quarantining individual provided an anterior nares swab sample (Average Cq: 29.5, 28.4, 28.6 for Apartments A, B, and C respectively). Although apartments differed in size, floor plan, and features (furniture, appliances, etc.), similar features at similar densities were swabbed across all three (n=140,116,125).

Each sampled surface was swabbed twice in immediately adjacent locations: first with a swab premoistened and stored in 95% ethanol, then by a second swab premoistened and stored in a 0.5% SDS w/v solution (Supplementary Materials and Methods). Ethanol samples underwent 16S V4 rRNA gene amplicon (16S) sequencing, and SDS samples underwent RT-qPCR for SARS-CoV-2 detection. 16S sequences were demultiplexed, quality filtered, and denoised with deblur (14) in Qiita (15) (Study ID:13957) using default parameters. Resulting feature tables were processed using QIIME2 (16).

4.2. Findings

We collected 381 matched 16S and SARS-CoV-2 surface samples from the three apartments, of which 178 (47%) were positive for SARS-CoV-2 (Fig. 4.1) (Sup. Table S1). Apartments A and C had comparable positivity rates (53% and 61%, respectively), but Apartment B was substantially lower (24%). In all three apartments, the rate of detection was highest in the bedroom (72% on average vs 47% overall). The swabbed surfaces were grouped into three categories: high-touch, low-touch, or floors. High-touch surfaces include door handles, switches, and countertops while walls, door faces, and ceiling fans are examples of low-touch surfaces. High-touch surfaces and floors had positivity rates 2-3 times higher than low-touch surfaces across all apartments (Sup. Table S2).

Figure 4.1. Distribution of SARS-CoV-2 viral load in isolation dorm apartments. (A-C) Floor plans for each apartment highlighting where SARS-CoV-2 RNA signatures were detected. (Inset) 3D rendering of the kitchen in Apartment C showing SARS-CoV-2 viral load in Genomic Equivalents (GEs) mapped to features in that room.

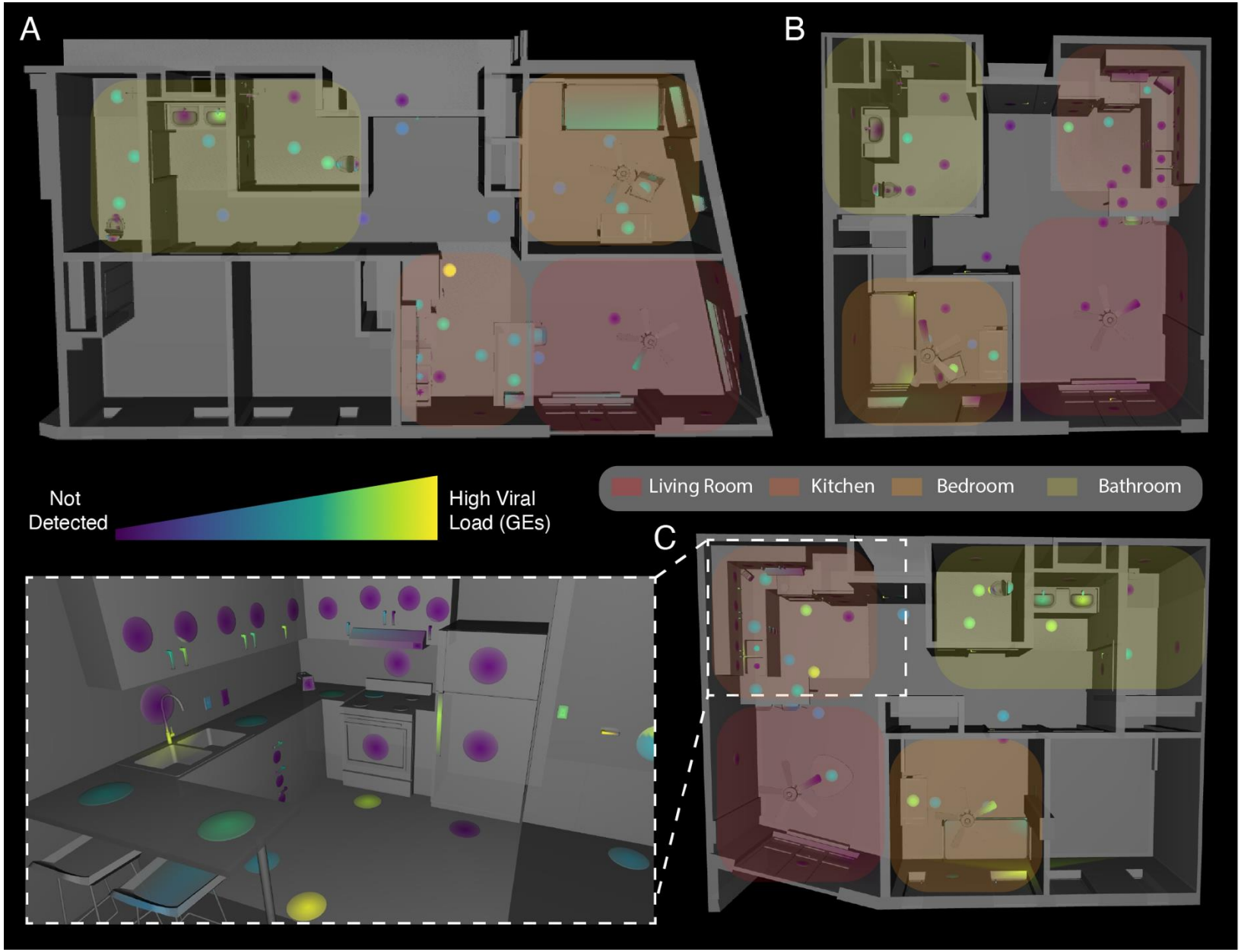
A
B
C
Not Detected
High Viral Load (GEs)
Living Room
Kitchen
Bedroom
Bathroom

We estimated surface viral load, in viral Genomic Equivalents (GE's), from Cq's using published regression curves (17) and mapped resulting viral loads onto 3D renderings of each apartment. High-touch surfaces had the highest viral load across all apartments, followed by floor samples and then high-use objects (fridge, sinks, toilets, beds) (Fig. 4.1). The maps for each apartment were studied to understand patterns of SARS-CoV-2 detection and deposition by room use. In the kitchens, objects with planar faces and handles, such as the refrigerator, cabinets, and drawers, revealed that only the touched handles had detectable RT-qPCR signal (Fig. 4.1C inset, as an example). We could not detect viral RNA on adjacent planar faces, which were presumably breathed on but not touched.

For quality control of 16S sequencing from low-biomass samples, we sequenced surface swabs from the apartments together with positive and negative controls using KatharoSeq (Supplementary Materials and Methods) (Sup. Fig. AD.1.2A) (18). Of 381 samples that underwent 16S sequencing, 121 fell below the KatharoSeq threshold and were excluded (Sup. Fig. AD.1.S2C). Informed by alpha rarefaction curves (Sup. Fig. AD.2.S2B), remaining samples were rarefied to 4000 features [sub-operational-taxonomic-units (sOTUs) (14)], removing an additional 36 samples from the analysis. Therefore, 157 samples were excluded from downstream analyses (122 SARS-CoV-2 negative matched swabs, 35 positive) (Sup. Fig. AD.2.S2C).

Bacterial alpha diversity analysis revealed a significant difference in Faith's phylogenetic diversity (Faith's PD) metric between SARS-CoV-2 detection status groupings at whole dataset level, but limited significant differences within apartments or

room types (Sup. Fig. AD.2.S3). Forward stepwise redundancy analysis (RDA) using the unweighted UniFrac beta diversity metric identified four non-redundant variables of significant effect size (apartment, surface material, type of room, and SARS-CoV-2 detection status) which accounted for 45.4% of the variation in the data (Sup. Fig. AD.2.4B). Analyzed by apartment, only in apartment B did virus detection lack significant effect. When subsetting the entire dataset by room type, detection status had a significant effect on variability across all rooms.

To test whether the bacterial community predicted SARS-CoV-2 status, we built a random forest classifier using rarefied sOTU data. The overall Area Under the Precision-Recall Curve (AUPRC) was 0.78, suggesting a statistically significant association, but insufficiently strong to predict SARS-CoV-2 status of a single sample from the bacterial community (Fig. 4.2A-B). We also applied compositionally aware, multinomial regression to our dataset to identify differentially abundant microbes between SARS-CoV-2 status groups (19). Because this regression model implicitly accounts for variable sequencing depth by modeling the relative log-fold-change of each feature in centered log-ratio (CLR) coordinates (20), we used unrarefied data as an input exclusively for this method (details in Materials and Methods). The top 32 features identified by the random forest classifier and the ranked log-fold-changes in feature abundance from the multinomial regression are shown in Figure 2C. Agreeing with previously published findings, *Rothia dentocariosa* was one of the top features identified by the classifier and was relatively positively associated with SARS-CoV-2 positive samples in the regression (8,12). Six sOTUs belonging to members of the genus *Corynebacterium* were also highly ranked as predictive for positive samples (Fig. 4.2C).

Figure 4.2. Analysis of microbial features associated with SARS-CoV-2 signatures. (A) Area under the precision-recall curve showing the overall prediction performance of the random forest classifiers when trained on the features from two apartments and cross validated on the remaining apartment. (B) Confusion matrix showing per-room type classifiers' performances (AURPC) when cross-applied on the remaining room types. The diagonal represents self validation. (C) Phylogenetic tree visualization (EMPress) where the differentially-abundant features between SARS-CoV-2 status groups identified by multinomial regression (Songbird) are plotted on the inner ring (red: positive log-fold-change in SARS-CoV-2 positive group, blue: negative log-fold-change in SARS-CoV-2 positive group), and the ranked sOTUs (top 32) identified as important by the random forest classifier are indicated on the outer ring. Leaves of the phylogenetic tree represent sOTUs relevant to the microbiome diversity and differential abundance analyses (number of sOTUs = 1047). The taxonomic classification (p_:phylum) of the sOTUs is indicated as colored branches in the phylogenetic tree.

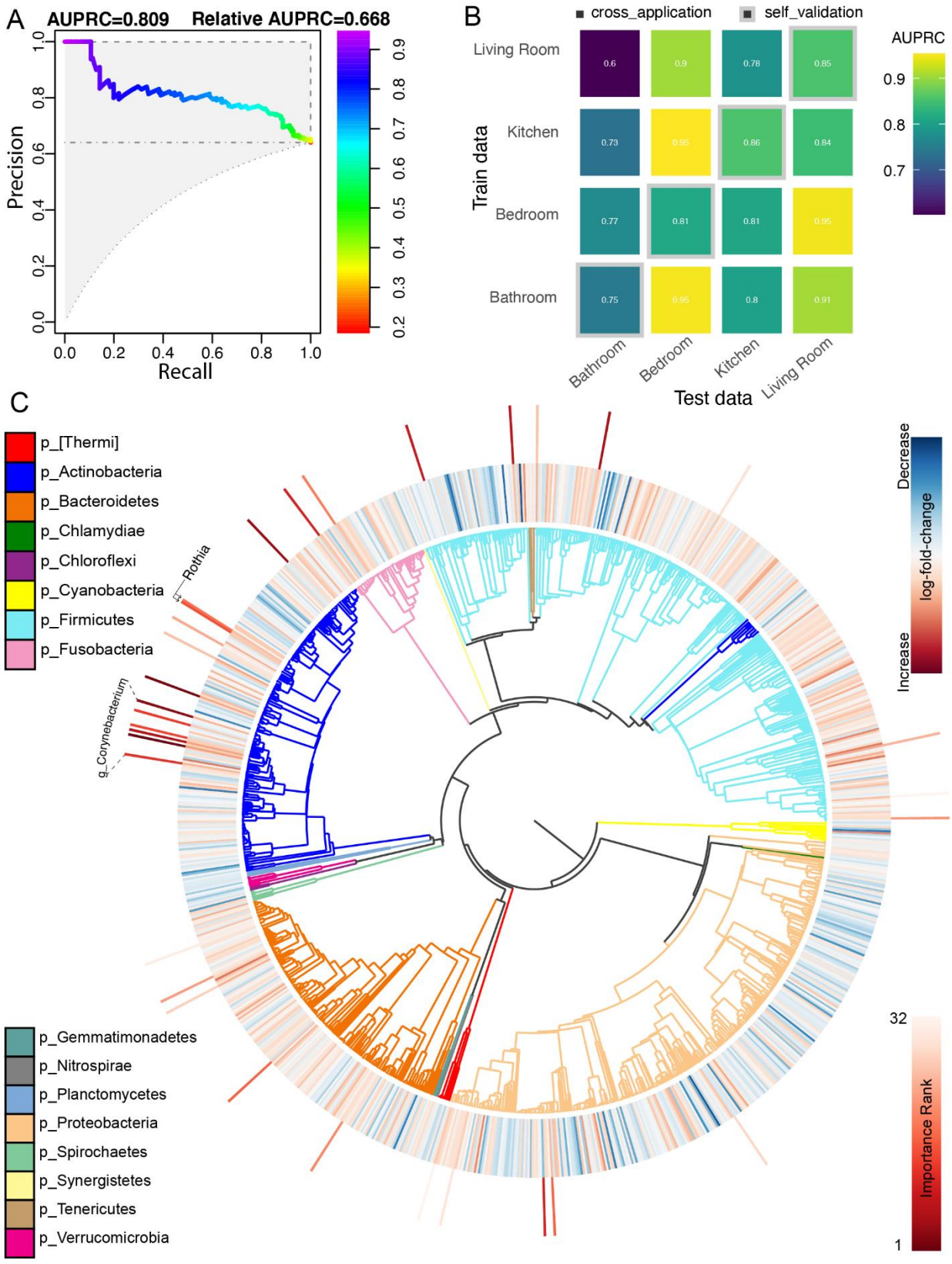
A
AUPRC=0.809
Relative AUPRC=0.668
Precision
Recall
B
cross_application
self_validation
Living Room
Kitchen
Bedroom
Bathroom
Train data
Test data
AUPRC
C
p_[Thermi]
p_Actinobacteria
p_Bacteroidetes
p_Chlamydiae
p_Chloroflexi
p_Cyanobacteria
p_Firmicutes
p_Fusobacteria
p_Gemmatimonadetes
p_Nitrospirae
p_Planctomycetes
p_Proteobacteria
p_Spirochaetes
p_Synergistetes
p_Tenericutes
p_Verrucomicrobia
g_Rothia
g_Corynebacterium
Decrease
log-fold-change
Increase
Importance Rank
32
1

Our results show that detailed spatial mapping of SARS-CoV-2 RNA abundance and associated bacterial signatures from built environment surfaces provides useful insight into potential sampling locations and associations between the viral and bacterial components of the microbiome. In the residential setting, high-touch surfaces have especially high viral loads, although confirming this with detailed spatial maps in other settings (hospitals, isolation hotels, schools) may be useful for guiding sampling designs. However, while high-touch surfaces have higher viral loads, floors had the highest rate of positivity, effectively rendering both floors and high-touch surfaces as good candidates for detecting SARS-CoV-2 indoors. We note that sensitivity of arbitrary single surface sampling to detect presence of even an unmasked COVID-19 patient is low, which was clearly evidenced in Apartment B where approximately only 1 in 4 random surface samples returned a SARS-CoV-2 detection event, so multiple samples or samples from selected surfaces should be collected. Although Apartment B had a considerably lower rate of positivity, trends of SARS-CoV-2 detection across indoor spaces and surface types closely mirrored those seen in the other two apartments in this study, and largely agree with other surveys of SARS-CoV-2 RNA traces in the residential setting (5-6). These results reinforce the utility of surface monitoring as a robust, cost-effective method for locating SARS-CoV-2 signals in the environment.

Our findings also corroborate SARS-CoV-2 associated changes in the microbiome published previously. *Rothia dentocariosa* specifically has been identified across different sample types in diverse settings, although reasons for these associations remain unclear. We also see multiple sOTUs belonging to the genus Corynebacterium predictive of a SARS-CoV-2 detection event, in contrast to the results of another study that found

Corynebacterium significantly decreased in the oral microbiome of individuals with COVID-19 (11). We hypothesize that *Corynebacterium* signal in this study might be evidence of human skin contamination of indoor surfaces through contact (22 - 23), leading to SARS-CoV-2 deposition on surfaces. It has been established that the occupants of a room contribute to the environmental microbiota, but our findings are among the first to demonstrate that disease-associated changes in the microbiome are mirrored in the built environment.

4.3. Acknowledgments

This research was supported by NIH grant (K01MH112436) to RFM, and the County of San Diego Health and Human Services Agency (Contract 563236). We thank Min Yi Wu, Bing Xia, Daniel Maunder, Michal Machnicki, Bhavika K. Kapadia, and Lizbeth Franco Vargas for their support with environmental SARS-CoV-2 detection as part of the EXCITE Lab, and Gail Ackermann for her help with sequence data deposition in Qiita and EBI.

Chapter 4, in full, is a reprint of the material as it appears in *mSystems*, “SARS-CoV-2 Distribution in Residential Housing Suggests Contact Deposition and Correlates with Rothia sp..” Cantú VJ, Salido RA, *et al*. The dissertation author was the primary investigator and first author of this paper.

4.4. References

1. Fielding-Miller R, Karthikeyan S, Gaines T, Garfein RS, Salido R, Cantu V, Kohn L, Martin NK, Wijaya C, Flores M, Omaleki V, Majnoonian A, Gonzalez-Zuniga P,

Nguyen M, Vo A V, Le T, Duong D, Hassani A, Dahl A, Tweeten S, Jepsen K, Henson B, Hakim A, Birmingham A, Mark AM, Nasamran CA, Rosenthal SB, Moshiri N, Fisch KM, Humphrey G, Farmer S, Tubb HM, Valles T, Morris J, Kang J, Khaleghi B, Young C, Akel AD, Eilert S, Eno J, Curewitz K, Laurent LC, Rosing T, SEARCH, Knight R. 2021. Wastewater and surface monitoring to detect COVID-19 in elementary school settings: The Safer at School Early Alert project. medRxiv 2021.10.19.21265226.

2. Jiang FC, Jiang XL, Wang ZG, Meng ZH, Shao SF, Anderson BD, Ma MJ. 2020. Detection of severe acute respiratory syndrome coronavirus 2 RNA on surfaces in quarantine rooms. Emerg Infect Dis 26:2162–2164.

3. Zhou J, Otter JA, Price JR, Cimpeanu C, Meno Garcia D, Kinross J, Boshier PR, Mason S, Bolt F, Holmes AH, Barclay WS. 2021. Investigating Severe Acute Respiratory Syndrome Coronavirus 2 (SARS-CoV-2) Surface and Air Contamination in an Acute Healthcare Setting During the Peak of the Coronavirus Disease 2019 (COVID-19) Pandemic in London. Clin Infect Dis 73:e1870–e1877.

4. Ben-Shmuel A, Brosh-Nissimov T, Glinert I, Bar-David E, Sittner A, Poni R, Cohen R, Achdout H, Tamir H, Yahalom-Ronen Y, Politi B, Melamed S, Vitner E, Cherry L, Israeli O, Beth-Din A, Paran N, Israely T, Yitzhaki S, Levy H, Weiss S. 2020. Detection and infectivity potential of severe acute respiratory syndrome coronavirus 2 (SARS-CoV-2) environmental contamination in isolation units and quarantine facilities. Clin Microbiol Infect 26:1658–1662.

5. Renninger N, Nastasi N, Bope A, Cochran SJ, Haines SR, Balasubrahmaniam N, Stuart K, Bivins A, Bibby K, Hull NM, Dannemiller KC. 2021. Indoor Dust as a Matrix for Surveillance of COVID-19. mSystems 6.

6. Maestre JP, Jarma D, Yu JRF, Siegel JA, Horner SD, Kinney KA. 2021. Distribution of SARS-CoV-2 RNA signal in a home with COVID-19 positive occupants. Sci Total Environ 778:146201.

7. Wu S, Wang Y, Jin X, Tian J, Liu J, Mao Y. 2020. Environmental contamination by SARS-CoV-2 in a designated hospital for coronavirus disease 2019. Am J Infect Control 48:910–914.

8. Marotz C, Belda-Ferre P, Ali F, Das P, Huang S, Cantrell K, Jiang L, Martino C, Diner RE, Rahman G, McDonald D, Armstrong G, Kodera S, Donato S, Ecklu-Mensah G, Gottel N, Salas Garcia MC, Chiang LY, Salido RA, Shaffer JP, Bryant MK, Sanders K, Humphrey G, Ackermann G, Haiminen N, Beck KL, Kim H-C, Carrieri AP, Parida L, Vázquez-Baeza Y, Torriani FJ, Knight R, Gilbert J, Sweeney DA, Allard SM. 2021. SARS-CoV-2 detection status associates with bacterial community composition in patients and the hospital environment. Microbiome 9:132.

9. Dunn RR, Fierer N, Henley JB, Leff JW, Menninger HL. 2013. Home Life: Factors Structuring the Bacterial Diversity Found within and between Homes. PLoS One 8:e64133.

10. Kembel SW, Jones E, Kline J, Northcutt D, Stenson J, Womack AM, Bohannan BJ, Brown GZ, Green JL. 2012. Architectural design influences the diversity and structure of the built environment microbiome. ISME J 6:1469–1479.

11. Lax S, Smith DP, Hampton-Marcell J, Owens SM, Handley KM, Scott NM, Gibbons SM, Larsen P, Shogan BD, Weiss S, Metcalf JL, Ursell LK, Vazquez-Baeza Y, Van Treuren W, Hasan NA, Gibson MK, Colwell R, Dantas G, Knight R, Gilbert JA. 2014. Longitudinal analysis of microbial interaction between humans and the indoor environment. Science (80-) 345:1048–1052.

12. Wu Y, Cheng X, Jiang G, Tang H, Ming S, Tang L, Lu J, Guo C, Shan H, Huang X. 2021. Altered oral and gut microbiota and its association with SARS-CoV-2 viral load in COVID-19 patients during hospitalization. npj Biofilms Microbiomes 7:61.

13. Gu S, Chen Y, Wu Z, Chen Y, Gao H, Lv L, Guo F, Zhang X, Luo R, Huang C, Lu H, Zheng B, Zhang J, Yan R, Zhang H, Jiang H, Xu Q, Guo J, Gong Y, Tang L, Li L. 2020. Alterations of the Gut Microbiota in Patients With Coronavirus Disease 2019 or H1N1 Influenza. Clin Infect Dis 71:2669–2678.

14. Amir A, McDonald D, Navas-Molina JA, Kopylova E, Morton JT, Zech Xu Z, Kightley EP, Thompson LR, Hyde ER, Gonzalez A, Knight R. 2017. Deblur Rapidly Resolves Single-Nucleotide Community Sequence Patterns. mSystems 2.

15. Gonzalez A, Navas-Molina JA, Kosciolek T, McDonald D, Vázquez-Baeza Y, Ackermann G, DeReus J, Janssen S, Swafford AD, Orchanian SB, Sanders JG, Shorenstein J, Holste H, Petrus S, Robbins-Pianka A, Brislawn CJ, Wang M, Rideout JR, Bolyen E, Dillon M, Caporaso JG, Dorrestein PC, Knight R. 2018. Qiita: rapid, web-enabled microbiome meta-analysis. Nat Methods 15:796–798.

16. Bolyen E, Rideout JR, Dillon MR, Bokulich NA, Abnet CC, Al-Ghalith GA, Alexander H, Alm EJ, Arumugam M, Asnicar F, Bai Y, Bisanz JE, Bittinger K, Brejnrod A, Brislawn CJ, Brown CT, Callahan BJ, Caraballo-Rodríguez AM, Chase J, Cope EK, Da Silva R, Diener C, Dorrestein PC, Douglas GM, Durall DM, Duvallet C, Edwardson CF, Ernst M, Estaki M, Fouquier J, Gauglitz JM, Gibbons SM, Gibson DL, Gonzalez A, Gorlick K, Guo J, Hillmann B, Holmes S, Holste H, Huttenhower C, Huttley GA, Janssen S, Jarmusch AK, Jiang L, Kaehler BD, Kang K Bin, Keefe CR, Keim P, Kelley ST, Knights D, Koester I, Kosciolek T, Kreps J, Langille MGI, Lee J, Ley R, Liu Y-X, Loftfield E, Lozupone C, Maher M, Marotz C, Martin BD, McDonald D, McIver LJ, Melnik A V., Metcalf JL, Morgan SC, Morton JT, Naimey AT, Navas-Molina JA, Nothias LF, Orchanian SB, Pearson T, Peoples SL, Petras D, Preuss ML, Pruesse E, Rasmussen LB, Rivers A, Robeson MS, Rosenthal P, Segata N, Shaffer M, Shiffer A, Sinha R, Song SJ, Spear JR, Swafford AD, Thompson LR, Torres PJ, Trinh P, Tripathi A,

Turnbaugh PJ, Ul-Hasan S, van der Hooft JJJ, Vargas F, Vázquez-Baeza Y, Vogtmann E, von Hippel M, Walters W, Wan Y, Wang M, Warren J, Weber KC, Williamson CHD, Willis AD, Xu ZZ, Zaneveld JR, Zhang Y, Zhu Q, Knight R, Caporaso JG. 2019. Reproducible, interactive, scalable and extensible microbiome data science using QIIME 2. Nat Biotechnol 37:852–857.

17. Salido RA, Cantú VJ, Clark AE, Leibel SL, Foroughishafiei A, Saha A, Hakim A, Nouri A, Lastrella AL, Castro-Martínez A, Plascencia A, Kapadia BK, Xia B, Ruiz CA, Marotz CA, Maunder D, Lawrence ES, Smoot EW, Eisner E, Crescini ES, Kohn L, Vargas LF, Chacón M, Betty M, Machnicki M, Wu MY, Baer NA, Belda-Ferre P, Hoff P De, Seaver P, Ostrander RT, Tsai R, Sathe S, Aigner S, Morgan SC, Ngo TT, Barber T, Cheung W, Carlin AF, Yeo GW, Laurent LC, Fielding-Miller R, Knight R. 2021. Analysis of SARS-CoV-2 RNA Persistence across Indoor Surface Materials Reveals Best Practices for Environmental Monitoring Programs. mSystems https://doi.org/10.1128/MSYSTEMS.01136-21.

18. Minich JJ, Zhu Q, Janssen S, Hendrickson R, Amir A, Vetter R, Hyde J, Doty MM, Stillwell K, Benardini J, Kim JH, Allen EE, Venkateswaran K, Knight R. 2018. KatharoSeq Enables High-Throughput Microbiome Analysis from Low-Biomass Samples. mSystems 3.

19. Morton JT, Marotz C, Washburne A, Silverman J, Zaramela LS, Edlund A, Zengler K, Knight R. 2019. Establishing microbial composition measurement standards with reference frames. Nat Commun 10:2719.

20. Quinn TP, Erb I, Gloor G, Notredame C, Richardson MF, Crowley TM. 2019. A field guide for the compositional analysis of any-omics data. Gigascience 8.

21. Bouslimani A, Porto C, Rath CM, Wang M, Guo Y, Gonzalez A, Berg-Lyon D, Ackermann G, Christensen GJM, Nakatsuji T, Zhang L, Borkowski AW, Meehan MJ, Dorrestein K, Gallo RL, Bandeira N, Knight R, Alexandrov T, Dorrestein PC. 2015. Molecular cartography of the human skin surface in 3D. Proc Natl Acad Sci U S A 112:E2120–E2129.

22. Byrd AL, Belkaid Y, Segre JA. 2018. The human skin microbiome. Nat Rev Microbiol 2018 163 16:143–155.

23. Cantrell K, Fedarko MW, Rahman G, McDonald D, Yang Y, Zaw T, Gonzalez A, Janssen S, Estaki M, Haiminen N, Beck KL, Zhu Q, Sayyari E, Morton JT, Armstrong G, Tripathi A, Gauglitz JM, Marotz C, Matteson NL, Martino C, Sanders JG, Carrieri AP, Song SJ, Swafford AD, Dorrestein PC, Andersen KG, Parida L, Kim H-C, Vázquez-Baeza Y, Knight R. 2021. EMPress Enables Tree-Guided, Interactive, and Exploratory Analyses of Multi-omic Data Sets. mSystems 6.

24. Protsyuk I, Melnik A V., Nothias LF, Rappez L, Phapale P, Aksenov AA, Bouslimani A, Ryazanov S, Dorrestein PC, Alexandrov T. 2017. 3D molecular cartography using LC–MS facilitated by Optimus and ’ili software. Nat Protoc 2017 131 13:134–154.

25. Hunter, J. D. Matplotlib: A 2D graphics environment. *Comput. Sci. Eng.* **9**, 90–95 (2007).

Appendix A. Supplemental Material for Chapter 1 Analysis of SARS-CoV2 RNA persistence across indoor surface materials reveals best practices for environmental monitoring programs

AA.1. Supplemental Figures

Figure A.A.1.S1. Comparison of signal persistence from heat-inactivated and untreated samples. (A) Swarm-plot showing distribution of average Cq of viral gene calls for acrylic and carpet (olefin) surfaces for both heat-inactivated and untreated samples. (B) Swarm plot comparing distribution of average Cq of viral gene class for heat-inactived or untreated samples. (C) Linear regression on Cqs from paired samples between heat-inactivated and untreated samples.

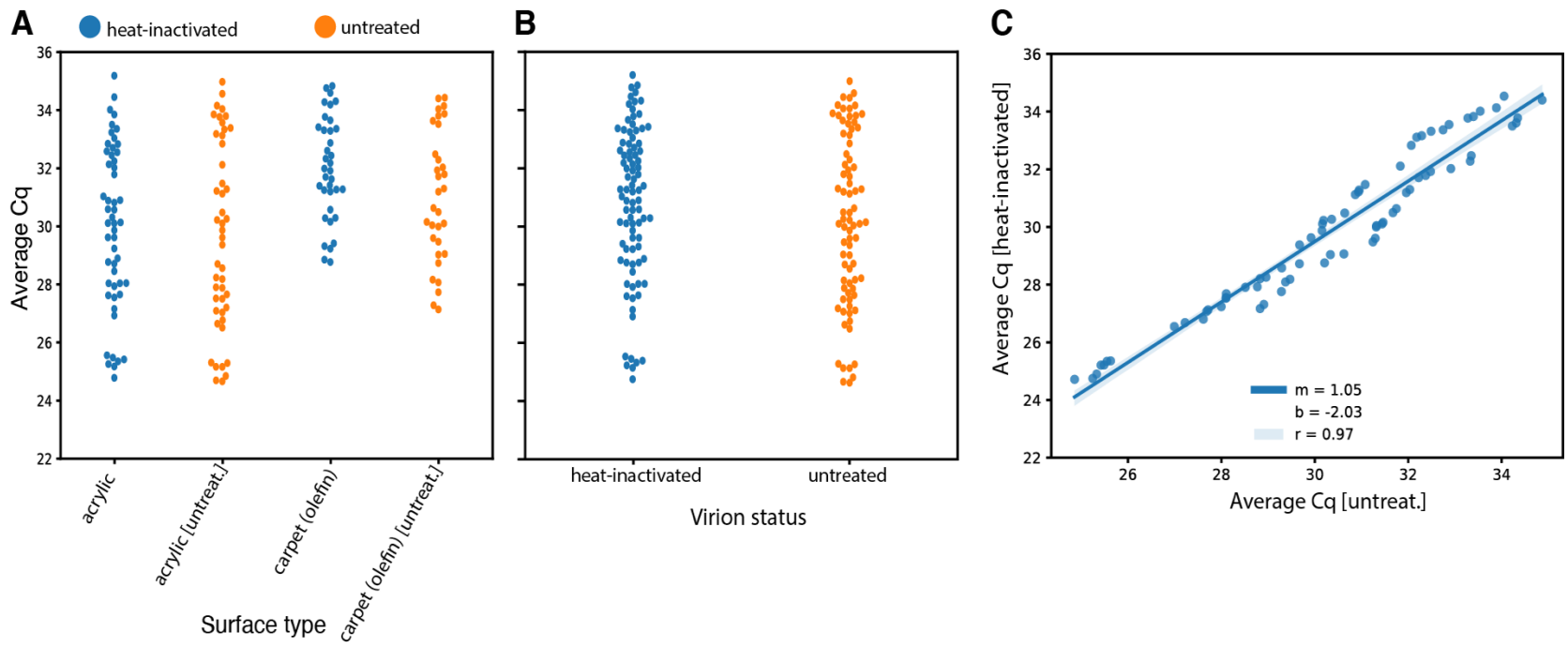
A
heat-inactivated
untreated
Average Cq
36
34
32
30
28
26
24
22
acrylic
acrylic [untreat.]
carpet (olefin)
carpet (olefin) [untreat.]
Surface type
B
heat-inactivated
untreated
Virion status
C
Average Cq [heat-inactivated]
Average Cq [untreat.]
m = 1.05
b = -2.03
r = 0.97

Figure AA.1.2. Lineplots showing the average Cq of RT-qPCR viral signals for Positive samples (circles) over seven days with overlaid scatterplots showing Cq for Inconclusive samples (diamonds). Inconclusive samples increase sensitivity of viral detection through surface swabs, seen as increased datapoints for low viral spike-ins in comparison to Positive samples alone. Viral spike-in concentrations reported as GE's from ddPCR.

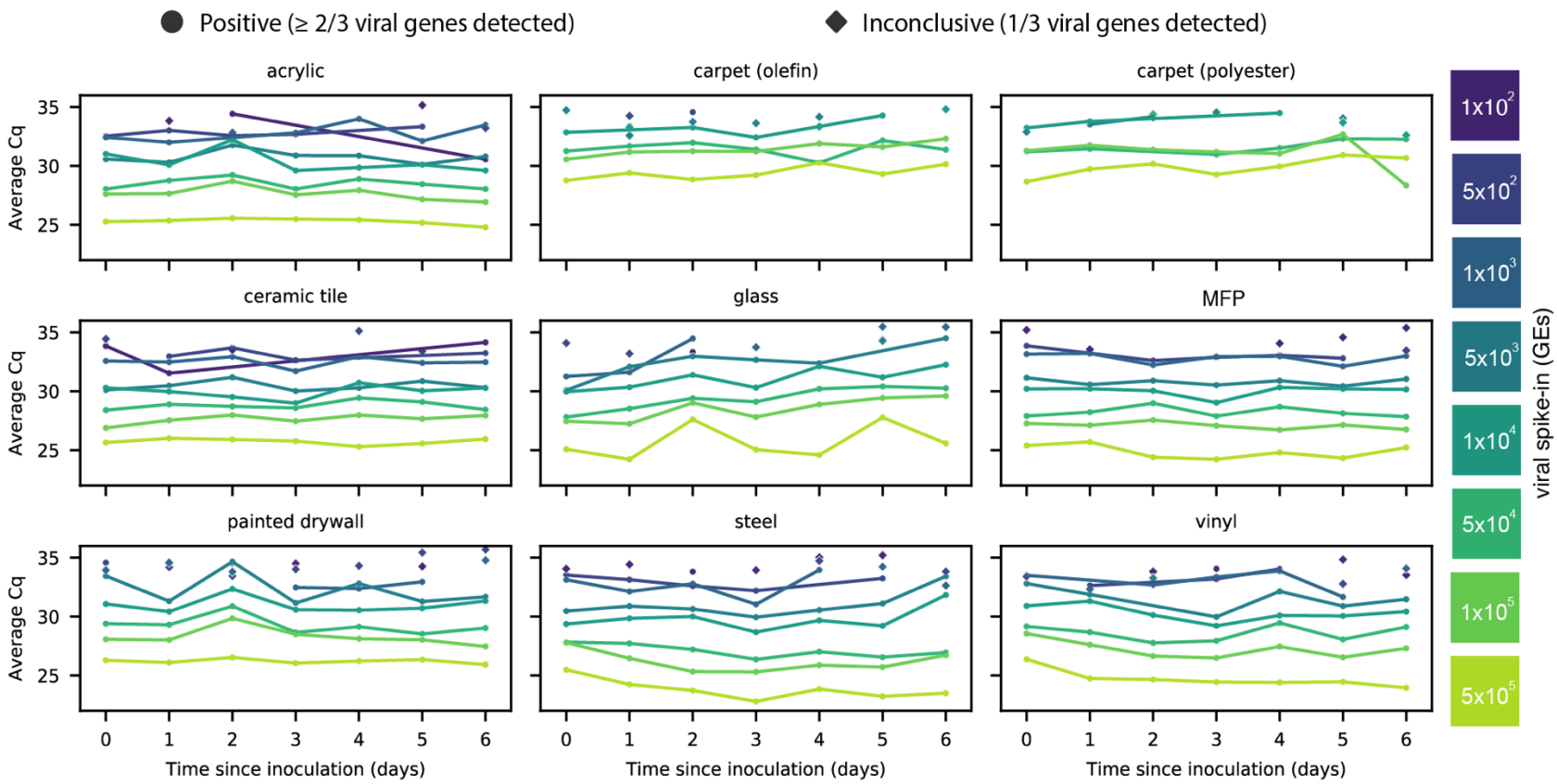
Positive (≥ 2/3 viral genes detected)
Inconclusive (1/3 viral genes detected)
acrylic
carpet (olefin)
carpet (polyester)
ceramic tile
glass
MFP
painted drywall
steel
vinyl
Average Cq
Time since inoculation (days)
viral spike-in (GEs)
1x10^2
5x10^2
1x10^3
5x10^3
1x10^4
5x10^4
1x10^5
5x10^5

AA.2. Supplemental Tables

Table AA.2.S1. Statistically significant differences from pairwise Mann-Whitney U tests between ranked values of average Cq from viral gene calls grouped by surface type after correction for multiple comparisons (** FDR-Benjamin/Hochberg, alpha = 0.005, N.s. = Not Significant)

Surface Type	carpet (olefin) [live]	carpet (olefin)	carpet (polyester)	ceramic tile	painted drywall	steel	vinyl	MDF	acrylic [live]	acrylic	glass
carpet (olefin)	N.s.										
carpet (olefin)[live]	N.s.	N.s.									
carpet (polyester)	N.s.	N.s.	N.s.								
ceramic tile	**	**	**	N.s.							
painted drywall	**	**	**	N.s.	N.s.						
steel	**	**	**	**	**	N.s.					
vinyl	**	**	**	N.s.	N.s.	N.s.	N.s.				
MDF	**	**	**	N.s.	**	N.s.	N.s.	N.s.			
acrylic [live]	**	**	**	N.s.	**	N.s.	N.s.	N.s.	N.s.		
acrylic	**	**	**	N.s.	**	N.s.	N.s.	N.s.	N.s.	N.s.	
glass	N.s.	**	**	N.s.	N.s.	N.s.	N.s.	N.s.	N.s.	N.s.	N.s.

Table AA.2.S2. Primer and probe sequences used for digital droplet PCR quantification of viral genome equivalents

Primer name	Modification	Sequence (5'-3')
COVID19_ORF1a-F		GTCGTAGTGGTGAGACACTTG
COVID19_ORF1a-R		GGCCACCAGCTCCTTTATTA
COVID19_ORF1a-Prb	FAM/ZEN/IBFQ	ATACCAGTGGCTTACCGCAAGGTT
RPP30-F		GATTTGGACCTGCGAGCG
RPP30-R		GCGGCTGTCTCCACAAGT
RPP30-Prb	HEX/ZEN/IBFO	CTGACCTGAAGGCTCT

Table AA.2.S3. Individual SARS-CoV-2 target gene positive criteria. Positive results were called on individual SARS-CoV-2 target genes that had a Cq of <37 with a confidence >0.7. A positive result on the extraction control gene (MS2) was called when it had a Cq of <37 with a confidence of >0.3.

Individual Target Passing Criteria		
Target	**Cq Range**	**Cq Confidence**
ORF1ab (viral)	<37	>0.7
N Gene (viral)	<37	>0.7
S Gene (viral)	<37	>0.7
MS2 (control)	<37	>0.3

Table AA.2.S4. RT-qPCR test result positive criteria. A Positive status was called for samples that had at least 2/3 positive calls on the SARS-CoV-2 target genes. An Inconclusive status was called on samples with only 1/3 positive calls on the SARS-CoV-2 target genes. A SARS-CoV-2 Detected result was called on samples where at least one out of three SARS-CoV-2 targets had a positive call; both Positive and Inconclusive status samples yielded SARS-CoV-2 Detected results. A Negative status was called on samples that had a positive call on the control gene and no positive calls on the SARS-CoV-2 target genes. An Invalid result was called when neither the control gene nor the viral target genes generated a positive call.

ORF1ab	**N Gene**	**S Gene**	**MS2**	**Status**	**Result**
Neg	Neg	Neg	Neg	Invalid	Invalid
Neg	Neg	Neg	Pos	Negative	SARS-CoV-2 Not Detected
Only one target=Pos			Pos/Neg	Inconclusive	SARS-CoV-2 Detected
Two or more Targets=Pos			Pos/Neg	Positive	SARS-CoV-2 Detected

A.A.3. Supplemental Information and Methods

Generation of Viruses

SARS-CoV-2 isolates USA-WA1/2020 (NR-52281) and Beta/B.1.351 hCoV-19/South Africa/KRISP-K005325/2020 (NR-54009) were obtained from BEI Resources. WA1 was propagated on VeroE6 cells. B.1.351 was passaged one time through primary bronchial epithelial cells differentiated at air-liquid interface (described below) to select against furin site mutations and then expanded on TMPRSS2-Vero cells (JCRB1819 established by Takeda, M., Sekisui XenoTech LLC). Viral genome copy number was determined by digital droplet PCR (ddPCR) of SARS-CoV-2 ORF1A performed by the Center for AIDS Research (CFAR) Genomics and Sequencing Core at UCSD. Heat inactivation was performed by incubating the virus at 65°C for 30 min. All work with SARS-CoV-2 was conducted in Biosafety Level-3 conditions at the University of California San Diego.

Bronchial epithelial cell culture and differentiation at air-liquid interface

Primary normal human bronchial epithelial cells (NHBECs) were acquired from Lonza (NHBE CC-2540; Walkersville, MD). The cell passage 1' frozen vial of NHBECs provided were tested and certified negative for HIV, HBV, HCV, sterility, and mycoplasma. NHBECs were revived from cryopreservation and expanded with PneumaCultTM Ex-Plus media (StemCell, 05040; Tukwila, WA). When cells were ~70-80% confluent, they were dissociated and seeded on collagen-coated transwells (Corning, 29442-082) pre-coated with 50 µg/mL Collagen type I from rat tail (BD Biosciences, 354236) at 7.5 µg/cm2.

Collagen-coated transwells were rehydrated with 100 µL PneumaCult TM Ex-Plus media at 37°C, 5% CO_2 for 30 minutes prior to seeding NHBECs for ALI culture. NHBECs were then seeded at 50,000 cells in 200 µL of media per collagen-coated transwell with 500 µL in the basolateral chamber. Media was changed on days 1 and 3 and then exchanged for PneumaCult TM ALI media (StemCell, 05021) supplemented with 10 µM ROCK inhibitor (Tocris, Y-27632) on day 4-7. Upon reaching confluency, approximately on Day 8, the apical media was removed, and the basal media replaced with PneumaCult TM ALI media without Y-27632. On the following day, the basal media was changed with fresh ALI media. Subsequent media changes were every 2-3 days. On Day 14 post-airlift, the apical surfaces were washed with DPBS, once per week. Cells were grown in 37°C, 5% CO_2 incubator until four weeks airlifted.

Infection of NHBECs at ALI

Prior to infection, apical chamber was incubated with two 30 min washes of PBS at 37°C, 5% CO2. Virus diluted in PBS was added to the apical chamber in 100uL and removed after 24h. Apical washes (150uL PBS with 10 min incubation at 37°C, 5% CO2,) were taken daily and stored at -80°C. Titer was determined by focus forming assay on TMPRSS2-Vero cells.

Digital droplet PCR

RNA was extracted using the QIAamp Viral RNA Mini kit (QIAGEN) following manufacturer's instructions. Equal volumes of RNA were run in triplicate and amplified in a 20 µL reaction (One-step RT-ddPCR Advanced Kit; Bio-Rad) with 900nM each primer

and 250nM probe_FAM/ZEN/IBFQ ORF1a with RNAse P as an internal control. Droplets were generated (QX200 droplet generator; Bio-Rad) and placed in ddPCR™ 96-Well Plates (Bio-Rad). Plates were heat-sealed and transferred to an Applied Biosystems Veriti 96 Well Thermal Cycler. PCR reaction conditions were 25°C for 3 min, 45°C for 60 min, 95°C for 10 min, and then cycled 45 times at 95°C for 30 sec, 60°C for 60 sec. Droplets were read on a QX200 droplet reader (Bio-Rad). The primers and probes use are described in Table A.A.2.S2.

Preparing Surfaces

The acrylic (Plaskolite, MC-05), carpets (olefin (TrafficMaster, 0701649510) and polyester (TrafficMaster, 7PD5N480144H)), ceramic tile (Daltile, MA031014HD1P2), glass (Gardner Glass Products, 11216), melamine-finished particleboard (MFP) (Roseburg, 371595), steel (M-D Building Products, 56020), and vinyl flooring (Lifeproof, I536111L) were purchased from a hardware store and used without modification. A slab of drywall (USG Sheetrock Brand, 141133) was painted with three coats of a white, matte interior paint and primer (Glidden, GLN9012N) and allowed to dry. Each of the nine surfaces were divided into 5 cm by 5 cm grids, sprayed with 70% v/v ethanol in water, and wiped down with a paper towel. The grid sections on the carpet materials were separated by 1 cm to prevent diffusion of the viral inoculum into neighboring sections.

Inoculating Surfaces

In both the heat-inactivated and untreated virus experiments, a concentrated stock of SARS-CoV-2 was diluted to create solutions with concentrations of $5x10^4$, $1x10^4$,

$5x10^3$, $1x10^3$, $5x10^2$, $1x10^2$, $5x10^1$, $1x10^1$ GEs/µL. A 10 µL volume of each solution was slowly dispensed onto a grid section while moving the pipette tip in a raster pattern in an attempt to evenly distribute the aliquot over each grid section's 25 cm^2 area. Water was dispensed in the same fashion onto sections that were swabbed each day as negative controls. The grid sections sampled for the first timepoint were allowed to dry for 1 hr before swabbing.

The surfaces inoculated with untreated virus were placed in tupperware containers in between inoculation and swabbing so that they could be safely stored outside of a biosafety cabinet. Surfaces inoculated with heat-inactivated virus were kept on designated bench tops without a container.

Swabbing

For each sample, a 1 mL sample collection tube (ThermoFisher Scientific, 3740TS) containing 800 µL of 0.5% w/v sodium dodecyl sulfate (SDS) (Acros Organics, 230420025) in water was prepared. This solution was chosen because 0.5% SDS has been shown to effectively inactivate amounts of SARS-CoV-2 used in this study after 30 minutes of contact time [**1, 2**]. To recover viral genetic material from the surface sections, a flocked swab (Affordable IHC Solutions) was pre-moistened with 0.5% SDS solution from a 1mL sample collection tube and the grid section was swabbed in a horizontal zig zag pattern, followed by a vertical zig zag pattern and finally, the same pattern in a diagonal orientation. The swab was rotated while swabbing and sufficient pressure was applied to maximize the contact surface area between the flocculated swab and the surface being swabbed. The flocculated end of the swab was placed back into the same

sample collection tube and the swab shaft was broken at the designated break point (3 cm break point). The 1D barcode of each tube was scanned using a handheld barcode scanner in order to link the sample to the experimental conditions of the swabbed surface.

Sample accession

Sample tubes were randomized and racked in barcoded 96-well tube racks (ThermoFisher Scientific, 4897). Sample identity was tracked using 2D barcodes at the bottom of each tube, which were scanned using a VisionMate Barcode Reader (ThermoFisher Scientific, 312800). A laboratory information management system (LIMS) was employed to track samples in multiwell plate formats using plate barcodes. [**3,4**]

Nucleic acid extraction

Individual 96-well tube racks were vortexed for 5 minutes to promote the suspension of viral particles from the swabs into the 0.5% SDS solution. Afterwards, 150 µL of the suspension buffer (0.5% SDS) were transferred with a multichannel pipette into barcoded deep well extraction plates and processed using the Omega MagBind Viral DNA/RNA kit (Omega Bio-Tek, M6246) on the Kingfisher Flex (ThermoFisher Scientific) platform following manufacturer's protocol with the following modifications: only 150µL of sample input was used (instead of the recommended 200µL) and 10 µL of MS2 phage was added to each well as an extraction control.

RT-qPCR (Multiplexed TaqPath)

Viral gene detection assays were performed using the RT-qPCR-based TaqPath™ COVID-19 Combo Kit (ThermoFisher Scientific, A47814) on a QuantStudio 7 Pro with a 384-well sample block (ThermoFisher Scientific) according to the manufacturer's protocol with the following modifications: 2 µL of purified RNA was added to a 1 µL reaction mix containing 0.75 µL TaqPath 4x Enzyme mix (ThermoFisher Scientific, A28523), 0.15 µL multiplex probe mix, and 0.1 µL nuclease free water, for a total reaction volume of 3 µL. Low volume transfers (< 5µL) were done with Mosquito HV Liquid Handlers (SPT Labtech). The following RT-qPCR cycling conditions were used: 25°C for 2 minutes, 53°C for 10 minutes, 95°C for 2 minutes, 55 cycles of 95°C for 3 seconds, and 60°C for 30 seconds. The signal was measured at the end of each 30 second interval at 60°C. Baseline determination and quantification cycle (Cq) signal determination were made using the Design and Analysis v2.4.3 software (Applied Biosystems) using the relative threshold (Crt) method. Positive calls for individual gene reporters were made according to Table AA.2.S3.

Because Inconclusive (only ⅓ viral target genes detected) samples allowed for increased sensitivity without considerable introduction of noise (Fig S2), the criteria for SARS-CoV-2 Detected results from surface swabs was defined as at least one out of three viral gene targets amplified. The US Food and Drug Administration has issued Emergency Use Authorization (EUA) for more than 150 RT-qPCR assays for the detection of SARS-CoV-2, the majority of which define a positive result as amplification in a single target [**5**]. The environmental surface swab result criteria used for this study is described in Table A.A.2.S4.

Controls

9 out of 81 (%11.1) blank surface swabs (surfaces inoculated with water) showed some viral signal. Contaminated blank surface swabs were exclusive to carpet (olefin), vinyl, acrylic, and MFP surface types, but not exclusive to any particular timepoint. All RT-qPCR positive controls behaved as expected. 2 out of 21 RT-qPCR negative controls failed to detect the extraction control (MS2 phage), but in both of those occasions, an alternative RT-qPCR negative control within the same RT-qPCR plate, respectively, yielded valid Not Detected results.

A.A.4. Supplemental References

1. Patterson EI, Prince T, Anderson ER, Casas-Sanchez A, Smith SL, Cansado-Utrilla C, Solomon T, Griffiths MJ, Acosta-Serrano Á, Turtle L, Hughes GL. 2020. Methods of Inactivation of SARS-CoV-2 for Downstream Biological Assays. J Infect Dis 222:1462–1467.

2. Welch SR, Davies KA, Buczkowski H, Hettiarachchi N, Green N, Arnold U, Jones M, Hannah MJ, Evans R, Burton C, Burton JE, Guiver M, Cane PA, Woodford N, Bruce CB, Roberts ADG, Killip MJ. 2020. Analysis of inactivation of SARS-CoV-2 by specimen transport media, nucleic acid extraction reagents, detergents, and fixatives. J Clin Microbiol 58.

3. Morgan SC, Aigner S, Anderson C, Belda-Ferre P, Hoff D, Marotz CA, Sathe S, Zeller M, Ahmed N, Audhya X, Baer NA, Barber T, Barrick B, Batachari L, Betty M, Blue SM, Brainard B, Buckley T, Case J, Chacón M, Cheung W, Chong L, Crescini ES, DeGrand S, Dimmock DP, Joelle Donofrio- J, Eisner ER, Estaki M, Franco Vargas L, Freddock M, Gallant RM, Galmozzi A, Gao NJ, Gilmer S, Grzelak EM, Hakim A, Hart J, Hobbs C, Humphrey G, Ilkenhans N, Jacobs M, Kahn CA, Kapadia BK, Kim M, Kurian S, Lastrella AL, Lawrence ES, Lee K, Liang Q, Liliom H, Sardo L, Logan R, Machnicki M, Magallanes CG, Malacki D, Marina RJ, Marsh C, Martin NK, Matteson NL, Maunder DJ, McBride K, McDonald B, Meadows AR, Meyer M, Morey AL, Mueller JR, Ngo TT, Nguyen J, Nguyen V, Nicholson LJ, Nouri A, Nunez E, Tyler Ostrander R, Pantham P, Park SS, Picone D, Plascencia A, Pratumchai I, Franc Ragsac M, Richardson AC, Robles-Sikisaka R, Ruiz CA, Ryan J, Sacco L, Saraf S, Seaver P, Smoot EW, Sweeney KM, Tekkatte C, Tsai R, Valentine H, Walsh S, Williams A, Yi Wu M, Xia B,

Yee B, Zhang JZ, Andersen KG, Farnaes L, Knight R, Laurent LC. 2021. Automated, miniaturized, and scalable screening of healthcare workers, first responders, and students for SARS-CoV-2 in San Diego County. medRxiv 2021.06.25.21257885.

4. Sathe S, Mah C, Ahmed N, Ragsac MF, Williams J, Yeo G. 2020. INSPECT sample tracking system Coronavirus Method Development Community https://doi.org/10.17504/protocols.io.bis8kehw.

5. MacKay MJ, Hooker AC, Afshinnekoo E, Salit M, Kelly J, Feldstein J V., Haft N, Schenkel D, Nambi S, Cai Y, Zhang F, Church G, Dai J, Wang CL, Levy S, Huber J, Ji HP, Kriegel A, Wyllie AL, Mason CE. 2020. The COVID-19 XPRIZE and the need for scalable, fast, and widespread testing. Nat Biotechnol. Nature Research.

Appendix B. Supplemental Material for Sentinel Cards Provide Practical SARS-CoV-2 Monitoring in School Settings

AB.1. Supplemental Figures

Figure AB.1.1. Diagram of sampling events for each day of the experiment. Each day the sentinel cards were swabbed pre- and post-inoculation and post wiping.

Measuring SARS-CoV-2 signal removal

Inoculate

Swab 1

Swab 2

Swab 3

Wipe

Appendix C. Supplemental Material for Implementation of Practical Surface SARS-CoV-2 Surveillance in School Settings

AC.1. Supplemental Figures

AC.2. Supplemental Tables

Table AC.2.S1. Average Cq of paired environmental samples from isolation rooms. The table shows the RT-qPCR results for the paired environmental samples (SDS, VTM) that were processed with the different combinations of extraction and RT-qPCR facility. The number of hits indicates how many gene targets were amplified during RT-qPCR.

RT-qPCR Facility		UCSD		County		UCSD		County	
		Avg Cq	# of Hits (out of 3)	Avg Cq	# of Hits (out of 2)	Avg Cq	# of Hits (out of 3)	Avg Cq	# of Hits (out of 2)
A	bathroom sink	25.41	3	28.67	2	29.50	3	30.71	2
	toilet floor	30.96	3	37.19	1	33.68	3	37.54	1
	bed headboard	29.47	2	Not Det.	0	Not Det.	0	Not Det.	0
	bedside floor	32.53	3	Not Det.	0	33.32	3	Not Det.	0
	bedside table	31.31	3	34.05	2	29.69	3	30.98	2
	kitchen sink handles	32.31	3	37.85	2	33.90	3	37.47	2
	kitchen table	33.92	3	39.23	1	32.26	3	33.61	2
	desk top	30.68	3	36.10	2	34.11	2	37.91	2
	desk chair	30.26	3	Not Det.	0	Not Det.	0	Not Det.	0
	light switch	28.06	3	37.92	1	Not Det.	0	41.24	1
B	bathroom sink	Not Det.	0	Not Det.	0	Not Det.	0	Not Det.	0
	bathroom door handle	Not Det.	0	Not Det.	0	Not Det.	0	Not Det.	0
	toilet floor	Not Det.	0	Not Det.	0	Not Det.	0	Not Det.	0
	bed headboard	Not Det.	0	Not Det.	0	Not Det.	0	Not Det.	0
	bedside floor	Not Det.	0	Not Det.	0	Not Det.	0	Not Det.	0
	bedside table	Not Det.	0	Not Det.	0	Not Det.	0	Not Det.	0
	kitchen counter	Not Det.	0	Not Det.	0	Not Det.	0	Not Det.	0
	kitchen sink handles	Not Det.	0	Not Det.	0	Not Det.	0	Not Det.	0
	coffee table	34.01	1	Not Det.	0	Not Det.	0	Not Det.	0
	light switch	Not Det.	0	Not Det.	0	35.42	1	38.74	2
C	bathroom sink	32.14	2	38.4	1	33.66	1	39.01	2
	toilet floor	33.75	2	Not Det.	0	Not Det.	0	36.78	2
	bed headboard	33.68	2	39.36	1	Not Det.	0	Not Det.	0
	bedside floor	Not Det.	0	Not Det.	0	Not Det.	0	37.91	1
	bedside table	31.71	3	39.4	1	31.41	3	32.64	2
	kitchen counter	32.36	3	Not Det.	0	Not Det.	0	38.44	2
	kitchen sink handles	31.11	3	38.755	2	33.13	2	39.38	1
	kitchen table	31.41	3	38.47	1	Not Det.	0	39.61	1
	desk top	30.67	3	37.035	2	31.35	3	32.35	2
	light switch	33.23	3	Not Det.	0	Not Det.	0	Not Det.	0

Table AC.2.S2. The standard surface sampling parameters are shown here. The UCSD based lab processed samples collected with SDS as the swabbing medium using a Thermo pipeline for RNA extraction and RT-qPCR. SDPHL however processes samples collected with VTM and uses the Perkin-Elmer pipeline for extracting RNA and performing RT-qPCR.

Lab	**Sample collection medium**	**RNA extraction**	**RT-qPCR**
UCSD	SDS	Thermo pipeline	Thermo pipeline
SDPHL	VTM	PerkinElmer pipeline	PerkinElmer pipeline

Table AC.2.S3. The 4 combinations of extraction and RT-qPCR facilities are shown here. The UCSD-based lab processed samples collected with SDS as the swabbing medium using a Thermo pipeline for RNA extraction and RT-qPCR. SDPHL however processes samples collected with VTM and uses the Perkin-Elmer pipeline for extracting RNA and performing RT-qPCR.

		Extraction Pipeline	
		Thermo (UCSD)	PerkinElmer (PHL)
RT-qPCR Pipeline	Thermo (UCSD)	Thermo	PE/Thermo
	PerkinElmer (PHL)	PE/Thermo	PE

Appendix D. Supplemental Material for SARS-CoV-2 Distribution in Residential Housing Suggests Contact Deposition and Correlates with Rothia sp.

AD.1. Supplemental Figures

Figure AD.1.S1. Timeline of events from first positive test to the end of the individual's quarantine period. Apartment C has no move in date because the individual quarantined in place.

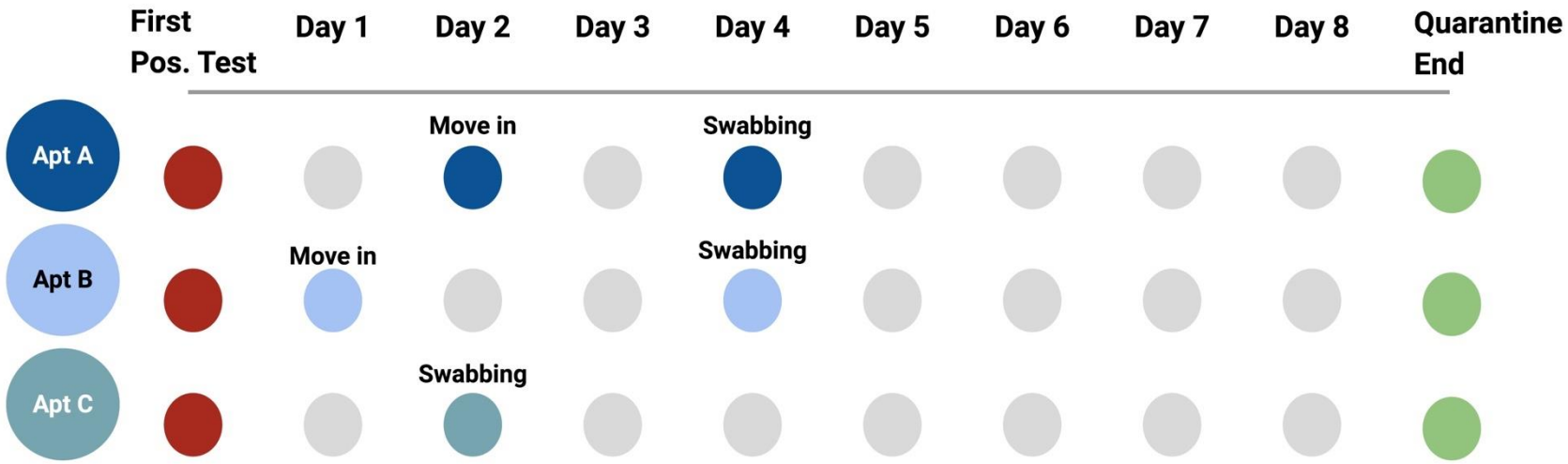
First Pos. Test
Day 1
Day 2
Day 3
Day 4
Day 5
Day 6
Day 7
Day 8
Quarantine End
Apt A
Move in
Swabbing
Apt B
Move in
Swabbing
Apt C
Swabbing

Figure AD.1.S2: Exclusion criteria for low biomass samples. (A) Diluted stock of a KatharoSeq positive control was sequenced along with the environmental samples and the resultant reads underwent pre-processing as detailed in the Supplementary Materials and Methods.The KatharoSeq Threshold (dashed lined), a minimum number of reads derived from a fitted allosteric sigmoidal curve, corresponds to a sequencing depth where at least 80% of the positive control reads are taxonomically classified to the appropriate target organisms (B) Top panel: Rarefaction curve showing observed features (alpha diversity metric) as a function of sequencing depth. Bottom panel: Graph showing how many samples would be included in downstream analysis as a function of rarefaction depth. (C) Table showing how many samples were removed at the KatharoSeq and Rarefaction thresholds and overall [(+) = SARS-CoV-2 positive, (-) = SARS-CoV-2 negative].

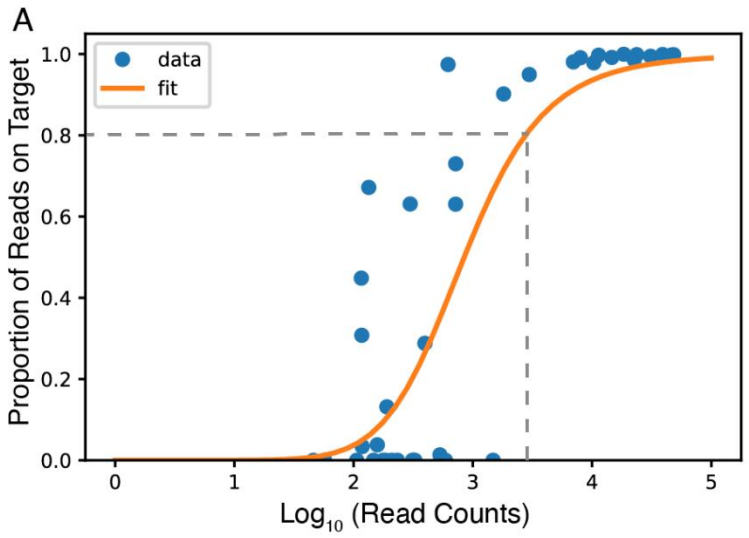

C

Apartment	Apt A		Apt B		Apt C		Total	
	+	-	+	-	+	-	+	-
Total Samples Sequenced	74	66	28	88	76	49	**178**	**203**
<KatharoSeq Threshold	6	30	14	55	2	14	**22**	**99**
<Rarefaction Threshold	5	5	6	11	2	7	**13**	**23**
Samples Removed	11	35	20	66	4	21	**35**	**122**
Samples Included	63	31	8	22	72	28	**143**	**81**

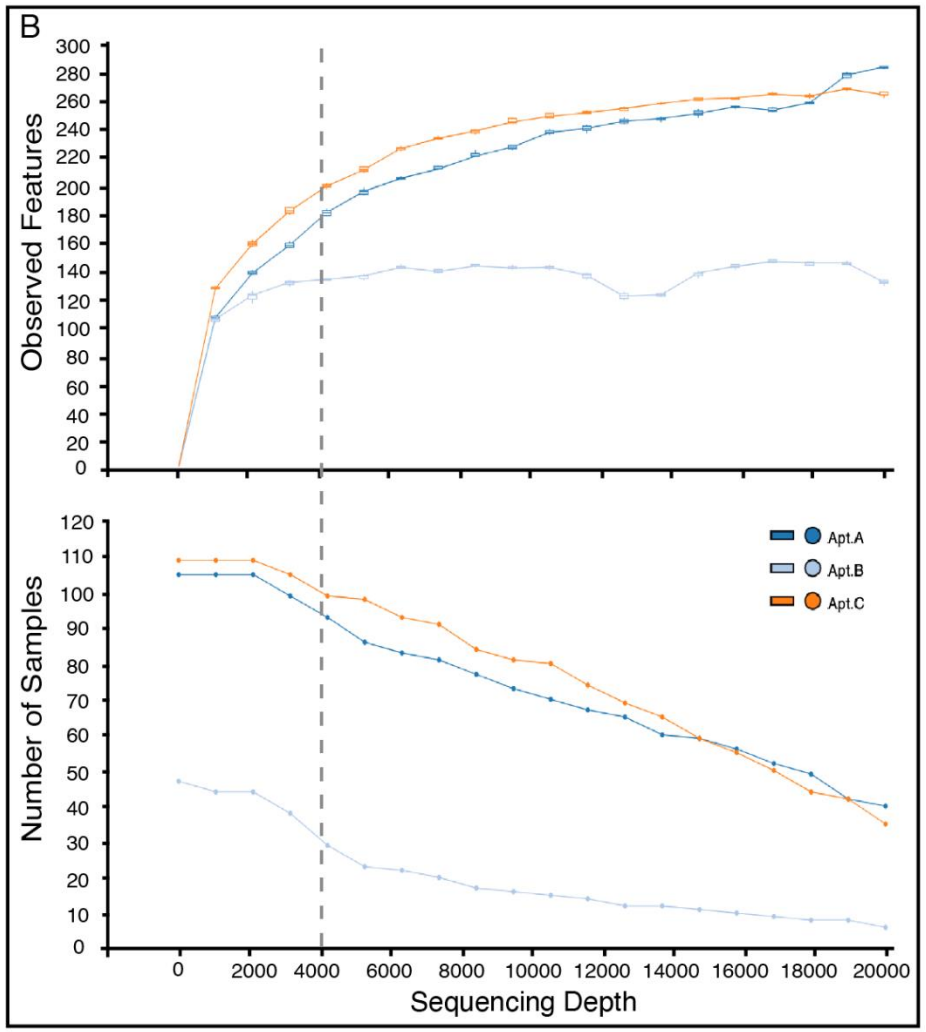

Figure AD.1.S3. Associations between microbial diversity and SARS-CoV-2 detection. (A) Mann-Whitney U test comparing ranked Faith's PD values from microbiome samples show a significant difference when grouped by SARS-CoV-2 status (U=7767, ***p=2.26x10-5). (B) When subsetting the samples by apartment, only apartment A shows a significant difference in Faith's PD values between SARS-CoV-2 status groups (**p≤0.001). (C) When subsetting the samples by room type, only the bedroom and kitchen show significant differences in Faith's PD values between SARS-CoV-2 status groups (*p≤0.01).

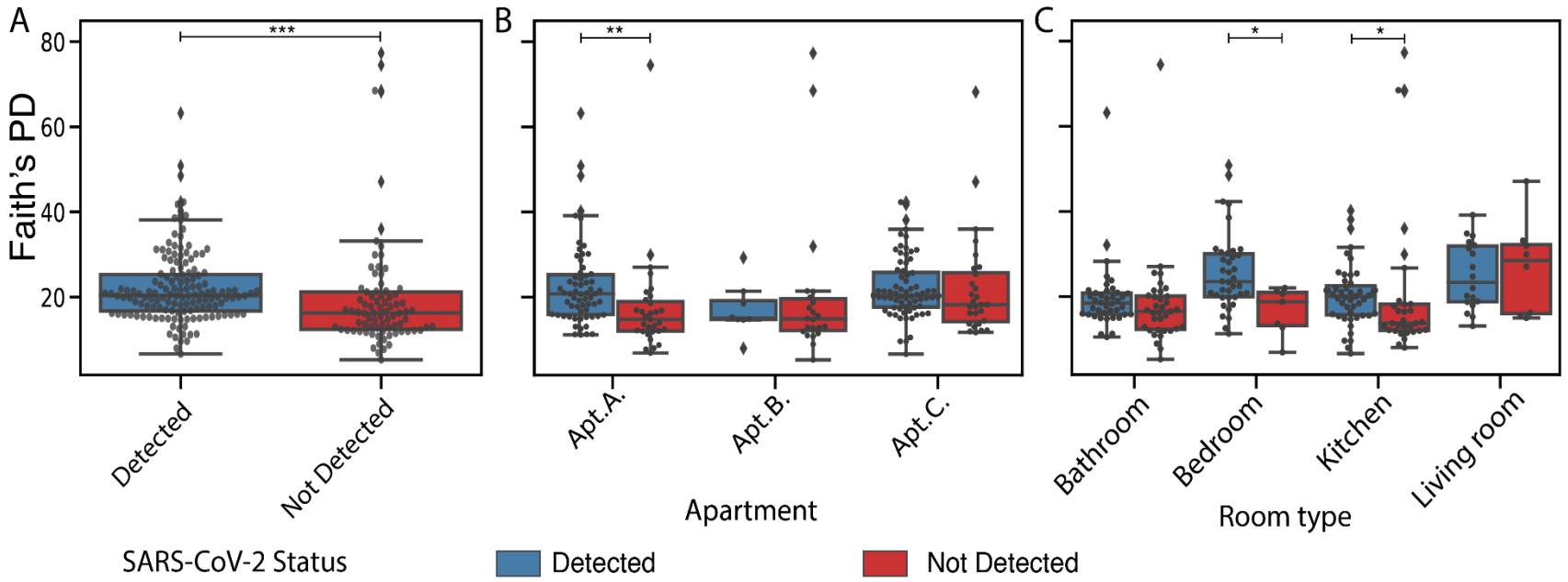
A
B
C
Faith's PD
80
60
40
20
***
**
*
*
Detected
Not Detected
Apt.A.
Apt.B.
Apt.C.
Apartment
Bathroom
Bedroom
Kitchen
Living room
Room type
SARS-CoV-2 Status
Detected
Not Detected

Figure AD.1.S4. Beta diversity analysis identifies the factors that contribute most to the separation of the data. (A) Principal coordinates analysis of the Unweighted Unifrac distance matrix shows that a major driver in the separation of this data is which apartment the samples came from. (B) Barplot showing the statistically significant effect sizes for non-redundant variables returned by RDA analysis. The largest effect size was explained by apartment (30.7%, p=0.0002), followed by surface material (10.7%, p=0.0002), room type (3.2%, p=0.0004), and SARS-CoV-2 detection status (0.84%, p=0.01).

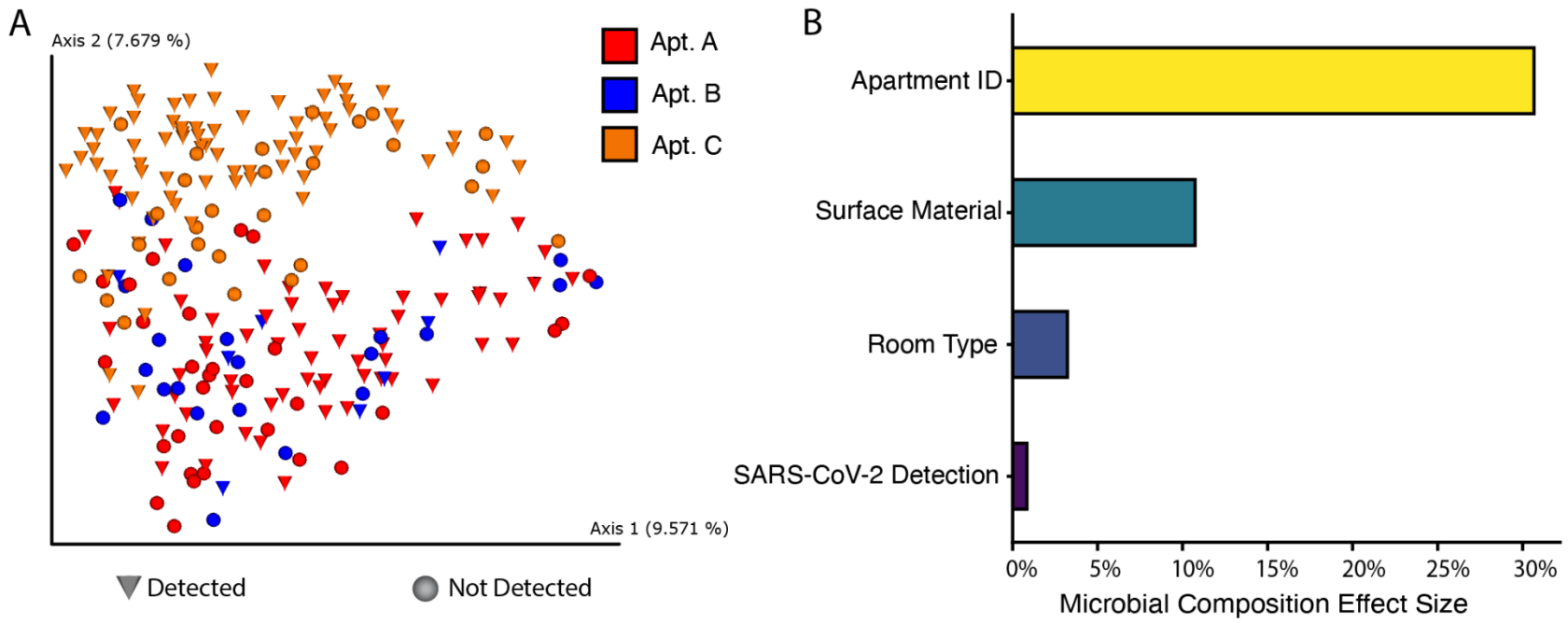
A
Axis 2 (7.679 %)
Axis 1 (9.571 %)
Apt. A
Apt. B
Apt. C
Detected
Not Detected
B
Apartment ID
Surface Material
Room Type
SARS-CoV-2 Detection
0%
5%
10%
15%
20%
25%
30%
Microbial Composition Effect Size

AD.2. Supplemental Tables

Table AD.2.S1. Environmental samples with detectable SARS-CoV-2 per apartment and room type.

Apartment	Room Type	Positives	Negatives	% Positive
A	Bathroom	19	21	48%
	Living Room	21	5	81%
	Kitchen	23	26	47%
	Living Room	11	14	44%
	Total	**74**	**66**	**53%**
B	Bathroom	4	20	17%
	Living Room	12	13	48%
	Kitchen	8	41	16%
	Living Room	4	14	22%
	Total	**28**	**88**	**24%**
C	Bathroom	22	14	61%
	Living Room	19	2	90%
	Kitchen	25	27	48%
	Living Room	10	6	63%
	Total	**76**	**49**	**61%**
ALL	**TOTAL**	**178**	**203**	**47%**

Table AD.2.S2. Environmental samples with detectable SARS-CoV-2 per apartment and surface type.

Apartment	*Surface Type*	*Positives*	*Negatives*	*% Positive*
A	*High Touch*	*42*	*27*	*61%*
	Low Touch	*17*	*36*	*32%*
	Floor	*15*	*3*	*83%*
B	*High Touch*	*18*	*38*	*32%*
	Low Touch	*5*	*42*	*11%*
	Floor	*5*	*8*	*38%*
C	*High Touch*	*47*	*12*	*80.0%*
	Low Touch	*19*	*35*	*35%*
	Floor	*10*	*2*	*83%*
ALL	*High Touch*	*107*	*77*	*58%*
	Low Touch	*41*	*113*	*27%*
	Floor	*30*	*13*	*70.0%*